Bulletin of the JSME Vol.7, No.2, 2020
Mechanical Engineering Journal

Numerical solutions for optimal double-mass dynamic vibration absorbers attached to a damped primary system

Toshihiko ASAMI* and Keisuke YAMADA**
* Department of Mechanical Engineering, University of Hyogo
2167 Shosha, Himeji, Hyogo, 671-2280, Japan
E-mail: asami@eng.u-hyogo.ac.jp
** Department of Mechanical Engineering, Kansai University
3-3-35 Yamate-cho, Suita, Osaka, 564-8680, Japan

Received: 20 January 2019; 7 January 2020; Accepted: 6 February 2020

Abstract
Because double-mass dynamic vibration absorbers (DVAs) are superior to single-mass DVAs in terms of their vibration suppression performance and robustness, they have been increasingly studied recently. The optimization of double-mass DVAs is much more difficult than that of single-mass DVAs. However, recently, the ability of formula manipulation solvers typified by *Mathematica* has greatly improved, and exact algebraic solutions have been obtained for double-mass DVAs. The optimal solution for a double-mass DVA attached to a damped primary system has been reported in the form of an exact algebraic solution in a previous report. That paper reported the algebraic optimal solutions for a series-type double-mass DVA for the compliance and mobility transfer functions of the primary system successfully obtained by applying three different optimization criteria: H_∞ optimization, H_2 optimization, and stability maximization. In the present article, the numerical solutions to optimization problems for double-mass DVAs that cannot be algebraically solved are presented. There are two types of double-mass DVAs: series- and parallel-type DVAs. When applying the three optimization criteria mentioned above to each of them, there exist a total of 22 different optimal solutions because there are three transfer functions— the compliance, mobility, and accelerance transfer functions—that are typically used to describe the absolute response of the primary system. Of these 22 solutions, 10 solutions for the compliance transfer function are introduced in this article.

Keywords : Vibration, Optimal design, Double-mass dynamic vibration absorbers, H_∞ optimization criterion, H_2 optimization criterion, Stability maximization criterion, Damped primary system

1. Introduction

A dynamic vibration absorber (DVA) is a small vibrating body attached to an object to suppress the vibrations of the object. Early DVAs did not include a damping mechanism, and their optimization criterion was extremely simple: the natural frequency of the DVA was made to coincide with that of the primary object (Frahm, 1911). Since the development of such early DVAs, it has become clear that the response of the primary system can be reduced not only in the vicinity of its resonance point but also over the entire frequency range when the DVA includes a damping mechanism (Ormondroyd and Den Hartog, 1928). There are now three representative optimization criteria for damped DVAs: H_∞ optimization, H_2 optimization, and stability maximization (Asami et al., 2002). Early damped DVAs were composed of a single mass, but research on DVAs composed of multiple masses has recently been carried out (Iwanami and Seto, 1984; Yasuda and Pan, 2003). When DVAs are multiplexed, it is expected that multiple vibration modes of the primary system can be suppressed and robustness against parameter fluctuation can be improved (Pan and Yasuda, 2005; Zuo, 2009). In this study, a multiplexed DVA was used to achieve improved vibration suppression performance, and the optimal design conditions for the simplest multiplexed DVA, the double-mass DVA, was investigated. Despite the double-mass DVA being the simplest multiplexed DVA, its optimization is very difficult because the number of parameters to be optimized increases from two for the single-mass case to five (Asami, 2017, 2018).

Paper No.19-00051
J-STAGE Advance Publication date : 13 February, 2020
[DOI: 10.1299/mej.19-00051]

Regarding the optimization of DVAs, particular interest has been paid to the design conditions for a special case in which there is no damping in the primary system. For example, as a typical H_∞ optimization criterion, Hahnkamm derived the optimal tuning condition of the DVA in 1932, and Brock then derived a formula for the optimal damping ratio in 1946. The optimization method they used is an approximation of the H_∞ optimization method proposed by Ormondroyd and Den Hartog in 1928, called the "fixed-point method." In 1997 and 2002, Nishihara (Nishihara and Matsuhisa, 1997; Nishihara and Asami, 2002) proposed an exact method of minimizing the H_∞ norm, which is the maximum amplitude of the response of the primary system; this method is hereafter called "Nishihara's method." Asami and Nishihara reported an exact algebraic solution using Nishihara's method for various transfer functions of the system in 2003. Regarding double-mass DVAs, the exact solutions based on the three optimization criteria have been reported by Asami (2017, 2018) and Nishihara (2017). All of these represent solutions for special cases in which there is no damping in the primary system. Although many researchers have sought general solutions in the case of a damped primary system, only numerical and perturbation solutions have been reported for optimization based on the H_∞ criterion (Ikeda and Ioi, 1978; Randall et al., 1981; Thompson, 1981; Soom and Lee, 1983; Sekiguchi and Asami, 1984). Surprisingly, exact algebraic solutions were found earlier for the double-mass DVA than for the single-mass DVA in the general case where there is damping in the primary system. In a previous study (Asami, 2019), for the mobility transfer function representing the absolute velocity response of the primary system subjected to force excitation, the H_∞-optimal solution of the series-type double-mass DVA was algebraically derived. The same paper presented an algebraic form of the H_2-optimal solution of a series-type double-mass DVA for the compliance transfer function representing the absolute displacement response of the primary system subjected to force excitation. Furthermore, with regard to the series-type double-mass DVA, an algebraic optimal solution has also been found for the stability maximization criterion, which is the third DVA optimization criterion.

There are two types of double-mass DVAs, the series-type and the parallel-type, and each can be classified as a force or motion excitation system depending on the excitation type. When there is no damping in the primary system, force and motion excitation systems have the same optimal solution, whereas including damping in the primary system causes them to have different optimal solutions. In addition, there are three typical transfer functions, called the compliance, mobility, and accelerance transfer functions, which are related to the absolute response of the primary system; thus, 22 different optimal solutions exist for the three types of optimization problems described above. (There is no solution to the accelerance transfer function in the H_2 criterion, and for the stability criterion, the solution does not depend on whether the system is a force or motion excitation system or which transfer function is used.) Among these solutions, algebraic forms have only been obtained in the three cases reported by Asami (2019), and exact solutions for the remaining 19 cases have not yet been obtained. The authors believe that it is necessary to derive the solutions for these unsolved optimization problems. Because all optimization problems involving double-mass DVAs can be reduced to solving simultaneous algebraic equations (Asami 2017; Asami et al., 2018), it is possible to solve the equations numerically.

This report presents the optimization of double-mass DVAs attached to a damped primary system based on the H_∞, H_2, and stability criteria using the compliance transfer function, which is the transfer function most frequently used in the field of mechanical vibration. The numerically determined optimal solutions for both the series- and parallel-type double-mass DVAs are also reported in this paper. Generally, the conventional fixed-point method cannot be used at all in the H_∞ optimization of multi-mass DVAs. Here, Nishihara's method (Nishihara and Matsuhisa, 1997; Nishihara and Asami, 2002) proves to be a powerful tool in this context.

2. Optimization problem for dynamic vibration absorbers attached to a damped primary system

Figures 1 and 2 show three-degree-of-freedom vibration systems consisting of two DVAs, A and B, attached in series and in parallel, respectively, to a primary system P with damping. Figures 1(a) and 2(a) show force excitation systems, in which the excitation force acts directly on the primary system, and Figs. 1(b) and 2(b) show motion excitation systems, in which the foundation of the system is displaced. Because these are linear systems, letting ω_1, ω_2, and ω_3 be the undamped natural angular frequencies of the primary system P and DVAs A and B, respectively, the ratio $|x_1/(f/k_1)|$ or $|x_1/x_0|$ of the amplitude of the steady-state response $x_1(t)$ to that of the sinusoidal input $f(t) = f_0 \sin \omega t$ or $x_0(t) = a_0 \sin \omega t$ can be fully represented by the following eight dimensionless parameters:

$$\lambda = \frac{\omega}{\omega_1},\ \mu = \frac{m_2 + m_3}{m_1},\ \mu_B = \frac{m_3}{m_2},\ \nu = \frac{\omega_2}{\omega_1},\ \nu_B = \frac{\omega_3}{\omega_2},\ \zeta_1 = \frac{c_1}{2m_1\omega_1},\ \zeta_2 = \frac{c_2}{2m_2\omega_2},\ \zeta_3 = \frac{c_3}{2m_3\omega_3} \tag{1}$$

where

$$\omega_1 = \sqrt{k_1/m_1},\quad \omega_2 = \sqrt{k_2/m_2},\quad \omega_3 = \sqrt{k_3/m_3}. \tag{2}$$

[DOI: 10.1299/mej.19-00051]

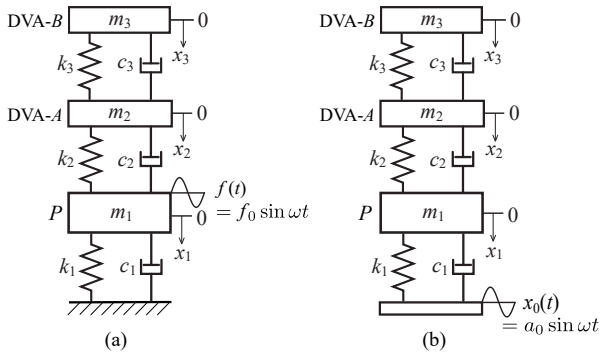

Fig. 1 Analytical model of a series-type DVA attached to a damped primary system subjected to (a) force or (b) motion excitation

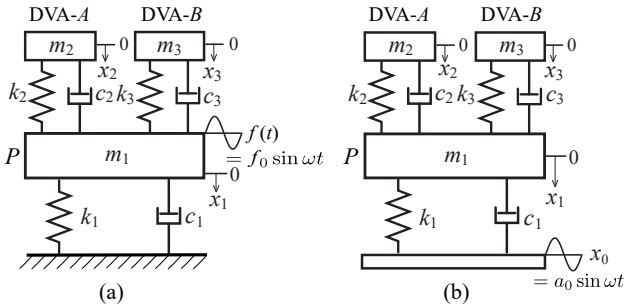

Fig. 2 Analytical model of a parallel-type DVA attached to a damped primary system subjected to (a) force or (b) motion excitation

It was assumed that λ varies from zero to infinity and a larger value of μ produces better DVA performance. When the mass ratio μ of the DVAs to the primary system and the value of the damping ratio ζ_1 for the primary system are given, the remaining five dimensionless parameters have optimal values. Determining these optimal values is the problem of optimizing the DVA for this system.

The symmetry of the parallel-type DVA shown in Fig. 2 means that a single optimal solution can be represented in two different forms by changing the assignment of the masses of DVA-*A* and DVA-*B*, which are known to have different masses in the optimal condition. In this report, DVA-*A* is defined as the larger DVA when the mass ratio μ is small.

As mentioned in the introduction, when there is damping in the primary system, the optimal values of the DVAs in the force excitation system (Figs. 1(a) and 2(a)) are different from those in the motion excitation system (Figs. 1(b) and 2(b)). Therefore, the optimization work was conducted separately for each system.

3. H_∞ optimization of series-type dynamic vibration absorber

3.1. H_∞ optimization for force excitation system

First, the optimization of the DVA was performed for the force excitation system shown in Fig. 1(a). Because the optimal damping ratio $\zeta_{2\mathrm{opt}}$ of DVA-*A* is known to be zero (Asami, 2017), if $c_2 = 0$ is set from the beginning, then the equations of motion of the system are

$$\left.\begin{aligned} &m_1\ddot{x}_1 + c_1\dot{x}_1 + k_1x_1 + k_2(x_1 - x_2) = f, \quad m_2\ddot{x}_2 + k_2(x_2 - x_1) + c_3(\dot{x}_2 - \dot{x}_3) + k_3(x_2 - x_3) = 0 \\ &m_3\ddot{x}_3 + c_3(\dot{x}_3 - \dot{x}_2) + k_3(x_3 - x_2) = 0. \end{aligned}\right\} \tag{3}$$

In the optimization of the compliance transfer function by the H_∞ criterion, the DVA is optimized by minimizing the resonance amplitude of the primary system, given by

$$h_{\max} = \left|\frac{x_1}{f/k_1}\right|_{\max}. \tag{4}$$

The minimized value of $h_{\max}$ is hereafter denoted $h_{\min}$. Because the vibratory system shown in Fig. 1(a) is a three-degree-of-freedom system, there are three resonance points in the vibration system unless the damping ratios for the subsystems are excessively large. First, the condition that the resonance points are equal in height gives the following three simultaneous algebraic equations (Asami et al., 2018):

$$\left.\begin{aligned} f_1 &= r - r^3 - 4r\zeta_1^2 + 4r\zeta_1^4 + \ll 86 \text{ terms} \gg + 4r\zeta_3^4\mu_B^5\nu^4\nu_B^4 = 0 \\ f_2 &= r^2 - r^3 - 2r^2\zeta_1^2 - 2r^2\zeta_3^2 + \ll 200 \text{ terms} \gg - 2\zeta_3^2\mu\mu_B^3\nu^4\nu_B^4 = 0 \\ f_3 &= 4r^4\zeta_3^2 - 4r^4\zeta_3^4 + 4r^4\zeta_3^2\mu_B - 4r^4\zeta_3^4\mu_B + \ll 83 \text{ terms} \gg + r^2\mu^2\mu_B\nu^4\nu_B^4 = 0. \end{aligned}\right\} \tag{5}$$

The symbol r used here represents a change of variable from the height $h_{\max}$ of the resonance point using the following equation:

$$r^2 = 1 - \frac{1}{h_{\max}^2}. \tag{6}$$

This variable conversion was carried out so that the terms of Eq. (5) do not include any fractional expressions. By this conversion, the problem of minimizing $h_{\max}$ is transformed into the problem of minimizing r. Hereafter, the minimum value of r is denoted $r_{\min}$.

[DOI: 10.1299/mej.19-00051]

In the H_∞ optimization of the series-type double-mass DVA, the number of parameters to be optimized is five (μ_B, ν, ν_B, ζ_3, and r). Therefore, the number of equations in Eq. (5) is two fewer than the number needed to solve this optimization problem. The remaining two equations are derived from the condition that minimizes the height of the resonance points adjusted to have equal heights by Eq. (5), given by

$$\mathrm{d}r = \frac{\partial r}{\partial \mu_B}\mathrm{d}\mu_B + \frac{\partial r}{\partial \nu}\mathrm{d}\nu + \frac{\partial r}{\partial \nu_B}\mathrm{d}\nu_B + \frac{\partial r}{\partial \zeta_3}\mathrm{d}\zeta_3 = 0. \tag{7}$$

This condition means that the total derivative of the parameter r, which represents the height of the resonance points, with respect to the four system parameters to be optimized should be zero (Asami et al., 2018). Because r is included in the functions f_1, f_2, and f_3, Eq. (7) can be rewritten as

$$\begin{bmatrix} \mathrm{d}r \\ \mathrm{d}r \\ \mathrm{d}r \end{bmatrix} = \begin{bmatrix} \dfrac{\partial r}{\partial f_1} & 0 & 0 \\ 0 & \dfrac{\partial r}{\partial f_2} & 0 \\ 0 & 0 & \dfrac{\partial r}{\partial f_3} \end{bmatrix} \begin{bmatrix} \dfrac{\partial f_1}{\partial \mu_B} & \dfrac{\partial f_1}{\partial \nu} & \dfrac{\partial f_1}{\partial \nu_B} & \dfrac{\partial f_1}{\partial \zeta_3} \\ \dfrac{\partial f_2}{\partial \mu_B} & \dfrac{\partial f_2}{\partial \nu} & \dfrac{\partial f_2}{\partial \nu_B} & \dfrac{\partial f_2}{\partial \zeta_3} \\ \dfrac{\partial f_3}{\partial \mu_B} & \dfrac{\partial f_3}{\partial \nu} & \dfrac{\partial f_3}{\partial \nu_B} & \dfrac{\partial f_3}{\partial \zeta_3} \end{bmatrix} \begin{bmatrix} \mathrm{d}\mu_B \\ \mathrm{d}\nu \\ \mathrm{d}\nu_B \\ \mathrm{d}\zeta_3 \end{bmatrix} = \begin{bmatrix} 0 \\ 0 \\ 0 \end{bmatrix}. \tag{8}$$

The 3×4 matrix in this equation is called the Jacobian matrix. For Eq. (8) to have a nontrivial solution, the rank of the Jacobian matrix must be less than or equal to 2 (Nishihara, 2017). Furthermore, for the rank drop condition of this matrix to be satisfied, the determinant of any 3×3 submatrix extracted from the Jacobian matrix must be zero: for example,

$$f_4 = \begin{vmatrix} \dfrac{\partial f_1}{\partial \nu} & \dfrac{\partial f_1}{\partial \nu_B} & \dfrac{\partial f_1}{\partial \zeta_3} \\ \dfrac{\partial f_2}{\partial \nu} & \dfrac{\partial f_2}{\partial \nu_B} & \dfrac{\partial f_2}{\partial \zeta_3} \\ \dfrac{\partial f_3}{\partial \nu} & \dfrac{\partial f_3}{\partial \nu_B} & \dfrac{\partial f_3}{\partial \zeta_3} \end{vmatrix} = 0, \quad f_5 = \begin{vmatrix} \dfrac{\partial f_1}{\partial \mu_B} & \dfrac{\partial f_1}{\partial \nu} & \dfrac{\partial f_1}{\partial \nu_B} \\ \dfrac{\partial f_2}{\partial \mu_B} & \dfrac{\partial f_2}{\partial \nu} & \dfrac{\partial f_2}{\partial \nu_B} \\ \dfrac{\partial f_3}{\partial \mu_B} & \dfrac{\partial f_3}{\partial \nu} & \dfrac{\partial f_3}{\partial \nu_B} \end{vmatrix} = 0. \tag{9}$$

The following fourth and fifth equations are obtained from expanding these determinants:

$$\left.\begin{aligned} f_4 &= -2r^6\zeta_1\zeta_3^2\mu\mu_B\nu^3 + 2r^7\zeta_1\zeta_3^2\mu\mu_B\nu^3 + \ll 11768 \text{ terms} \gg - 8r^4\zeta_3^7\mu\mu_B^{11}\nu^8\nu_B^{11} = 0 \\ f_5 &= 8r^6\zeta_1\zeta_3^3\mu\mu_B\nu^3 - 8r^7\zeta_1\zeta_3^3\mu\mu_B\nu^3 + \ll 18655 \text{ terms} \gg + 64r^4\zeta_3^8\mu\mu_B^{10}\nu^8\nu_B^{11} = 0. \end{aligned}\right\} \tag{10}$$

There are several ways to select a submatrix, and different equations from those given in Eq. (10) are derived depending on the way selected. However, we have confirmed that the choice does not affect the final solution value. This means that as long as the rank drop condition is satisfied, the choice of submatrix is arbitrary.

In the simultaneous algebraic equations composed of the formulas given in Eqs. (5) and (10), when the values of μ and ζ_1 are given, the five unknown parameters (μ_B, ν, ν_B, ζ_3, and r) can be solved using the Newton–Raphson method in *Mathematica* ver.11.3 from a suitable starting point for these parameters. Thus, the optimal values $\mu_{B\mathrm{opt}}$, ν_{opt}, $\nu_{B\mathrm{opt}}$, and $\zeta_{3\mathrm{opt}}$ of the DVA parameters and the minimum value $r_{\min}$ representing the height of the resonance points can be obtained. The minimized resonance amplitude $h_{\min}$ is then calculated as

$$h_{\min} = \sqrt{\frac{1}{1 - r_{\min}^2}}. \tag{11}$$

In a previous study by one of the authors on the H_∞ optimization of a single-mass DVA, the condition for equalizing the heights of the two resonance points was described by the simultaneous equations $f_1 = 0$ and $f_2 = 0$ (Asami and Nishihara, 2003). The height of the resonance points was then minimized by finding the multiple root of these simultaneous equations. Fortunately, a single quartic equation could be derived from these simultaneous equations, and the multiple root of the higher-order equation could be obtained from the condition that the determinant of the Sylvester matrix must be zero. However, the simultaneous equations given in Eq. (5) cannot be combined into a single equation; thus, the Sylvester matrix cannot be used in this case. However, the Jacobian matrix in Eq. (8) performs the same function as the Sylvester matrix. In other words, employing Eq. (7) or (8) is a process of searching for the multiple root of the simultaneous equations given in Eq. (5).

[DOI: 10.1299/mej.19-00051]

3.2. H_∞ optimization for motion excitation system

Next, the optimization of the DVA attached to the motion excitation system shown in Fig. 1(b) was performed. Here again, if $c_2 = 0$, then the equations of motion are

$$\left.\begin{aligned} &m_1\ddot{x}_1 + c_1(\dot{x}_1 - \dot{x}_0) + k_1(x_1 - x_0) + k_2(x_1 - x_2) = 0 \\ &m_2\ddot{x}_2 + k_2(x_2 - x_1) + c_3(\dot{x}_2 - \dot{x}_3) + k_3(x_2 - x_3) = 0, \quad m_3\ddot{x}_3 + c_3(\dot{x}_3 - \dot{x}_2) + k_3(x_3 - x_2) = 0. \end{aligned}\right\} \tag{12}$$

In the H_∞ optimization of a motion excitation system, the DVA is optimized by minimizing the maximum transmissibility. That is, the evaluation index is

$$h_{\max} = \left|\frac{x_1}{x_0}\right|_{\max}. \tag{13}$$

The following simultaneous algebraic equations with five unknowns can then be derived by the same procedure as for the force excitation system:

$$\left.\begin{aligned} f_1 &= r - r^3 - 4r^3\zeta_1^2 + 4r^5\zeta_1^4 + \ll 84 \text{ terms} \gg + 4r\zeta_3^4\mu_B^5\nu^4\nu_B^4 = 0 \\ f_2 &= r^2 - r^3 - 2r^4\zeta_1^2 - 2r^3\zeta_3^2 + \ll 197 \text{ terms} \gg - 2\zeta_3^2\mu\mu_B^3\nu^4\nu_B^4 = 0 \\ f_3 &= 4r^4\zeta_3^2 - 4r^4\zeta_3^4 + 4r^4\zeta_3^2\mu_B - 4r^4\zeta_3^4\mu_B + \ll 82 \text{ terms} \gg + r^2\mu^2\mu_B\nu^4\nu_B^4 = 0 \\ f_4 &= -2r^6\zeta_1\zeta_3^2\mu\mu_B\nu^3 + 2r^7\zeta_1\zeta_3^2\mu\mu_B\nu^3 + \ll 11768 \text{ terms} \gg - 8r^4\zeta_3^7\mu\mu_B^{11}\nu^8\nu_B^{11} = 0 \\ f_5 &= 8r^6\zeta_1\zeta_3^3\mu\mu_B\nu^3 - 8r^7\zeta_1\zeta_3^3\mu\mu_B\nu^3 + \ll 18655 \text{ terms} \gg + 64r^4\zeta_3^8\mu\mu_B^{10}\nu^8\nu_B^{11} = 0. \end{aligned}\right\} \tag{14}$$

Equation (14) can be numerically solved in the same way as Eqs. (5) and (10).

3.3. Optimal values of design parameters for dynamic vibration absorber

The H_∞-optimal design parameters for the DVA obtained by numerical analysis are shown in Fig. 3. As shown in the figure, the optimal values for the four design parameters of the DVA monotonically decrease or increase as the primary system damping increases. When considering the overall behavior of the parameters, the changes in their optimal values with respect to ζ_1 are smaller in the motion excitation system than in the force excitation system. It is noteworthy that ν_{opt} has been previously reported to monotonically increase in the H_∞-optimal solution to the optimization of the mobility transfer function (Asami, 2019), whereas ν_{opt} was found to decrease monotonically in the optimization of the compliance transfer function in the previous study, as shown in Fig. 3(b).

3.4. Minimized H_∞ performance index

In Fig. 4, panels (a) and (b) show the resonance amplitudes of the force and motion excitation systems, respectively, to which the series-type double-mass DVA optimized by the H_∞ criterion is attached. The curve for $\mu = 0$ shown in gray is the resonance amplitude for the primary system when no DVA is attached, which can be calculated from the following simple equations. First, for the force excitation system shown in Fig. 4(a),

$$h_{\min} = \frac{1}{2\zeta_1\sqrt{1-\zeta_1^2}}. \tag{15}$$

Second, for the motion excitation system shown in Fig. 4(b),

$$h_{\min} = \frac{1}{2\zeta_1}\sqrt{\frac{1 + 4\zeta_1^2 - 8\zeta_1^4 + \sqrt{1+8\zeta_1^2}}{2(1-\zeta_1^2)}}. \tag{16}$$

As shown in Fig. 4, the resonance point is kept low as the primary system damping ζ_1 increases and can be further suppressed by attaching the DVA. Furthermore, the values of $h_{\min}$ in the motion excitation system (Fig. 4(b)) are greater than those in the force excitation system (Fig. 4(a)) from when ζ_1 exceeds approximately 0.1.

3.5. Frequency response of the primary system with a series-type dynamic vibration absorber optimized by the H_∞ criterion

Figures 5 and 6 show the frequency response function for the system fitted with the series-type double-mass DVA optimized by the H_∞ criterion in the force and motion excitation systems, respectively, in the cases where the mass ratio of the DVA to the primary system is $\mu = 0.05$ and 0.1. As shown in these figures, the resonance is kept low as the primary system damping ζ_1 or the mass of the DVA increases. These curves are very similar to the frequency response function for a damped single-degree-of-freedom system but with three resonance points.

[DOI: 10.1299/mej.19-00051]

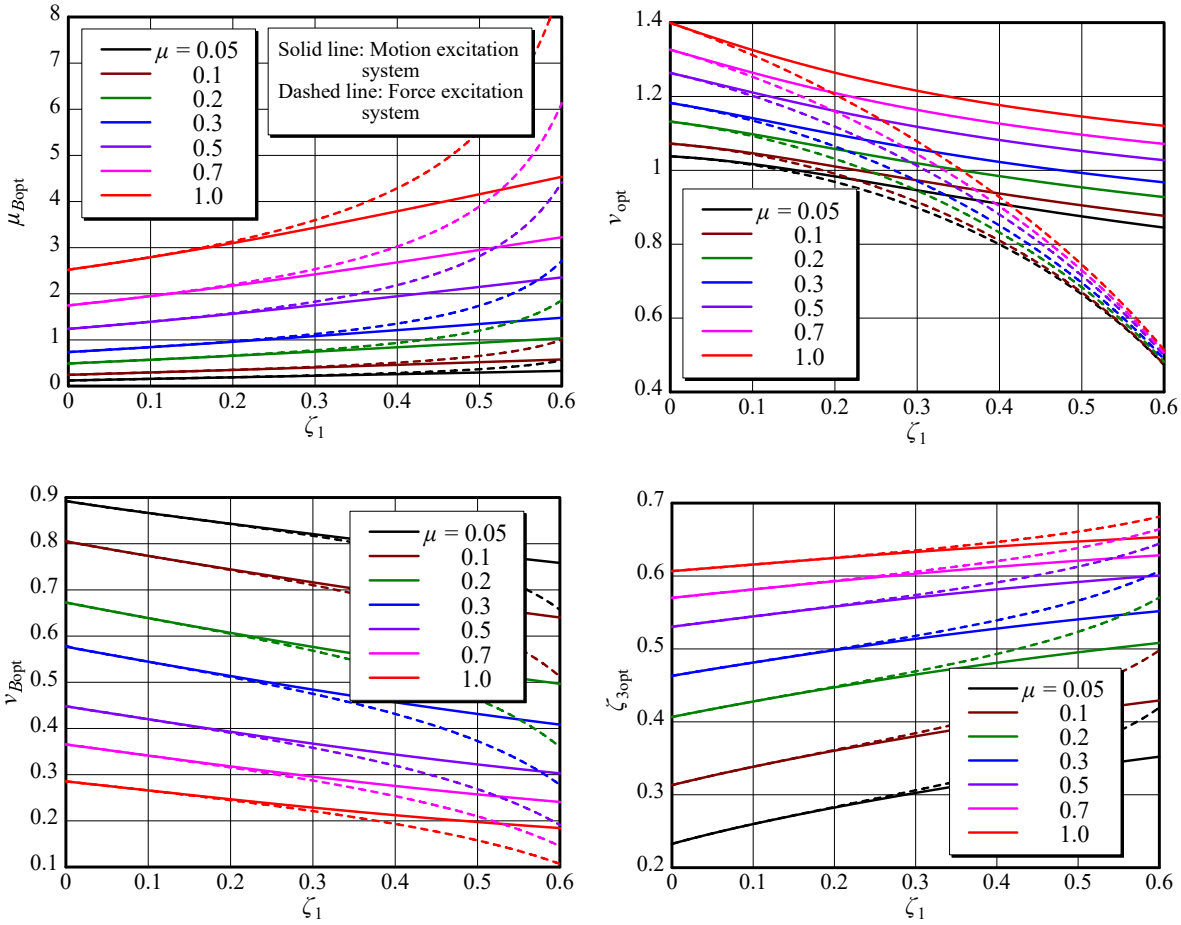

Fig. 3 H_∞-optimal solutions for the series-type DVA; (a) Optimal mass ratio $\mu_{B\mathrm{opt}}$; (b) Optimal tuning ratio ν_{opt}; (c) Optimal tuning ratio $\nu_{B\mathrm{opt}}$; (d) Optimal damping ratio $\zeta_{3\mathrm{opt}}$

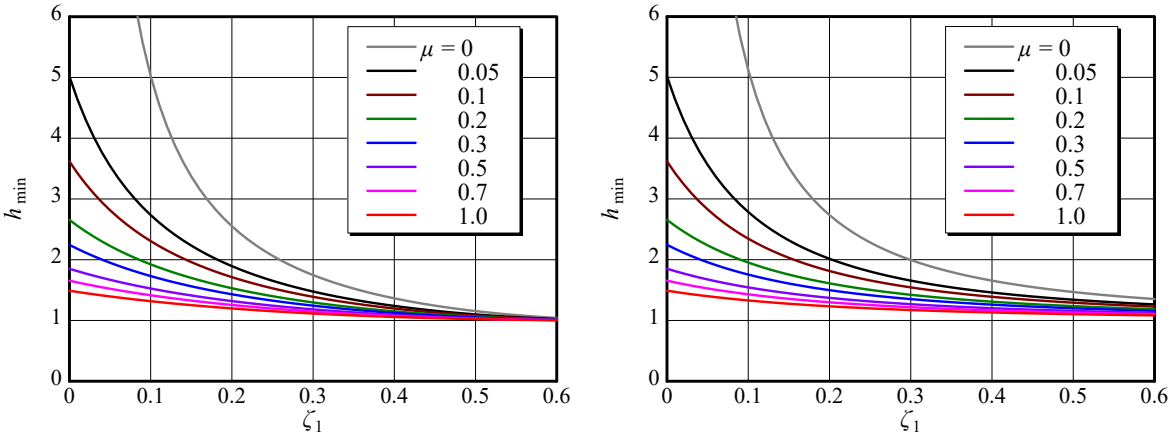

Fig. 4 Minimized response amplitude of primary systems fitted with the series-type DVA optimized by the H_∞ criterion; (a) Minimized amplitude $h_{\min}$ of the force excitation system; (b) Minimized amplitude $h_{\min}$ of the motion excitation system

4. H_∞ optimization of parallel-type dynamic vibration absorber

4.1. H_∞ optimization for force excitation system

When the damping coefficient c_2 of DVA-A is assumed to be nonzero, the equations of motion of the force excitation system shown in Fig. 2(a) are as follows:

$$\left.\begin{aligned} &m_1\ddot{x}_1 + c_1\dot{x}_1 + c_2(\dot{x}_1 - \dot{x}_2) + c_3(\dot{x}_1 - \dot{x}_3) + k_1x_1 + k_2(x_1 - x_2) + k_3(x_1 - x_3) = f \\ &m_2\ddot{x}_2 + c_2(\dot{x}_2 - \dot{x}_1) + k_2(x_2 - x_1) = 0, \quad m_3\ddot{x}_3 + c_3(\dot{x}_3 - \dot{x}_1) + k_3(x_3 - x_1) = 0. \end{aligned}\right\} \tag{17}$$

Here again, the following simultaneous algebraic equations are obtained from the condition that the heights of the three

[DOI: 10.1299/mej.19-00051]

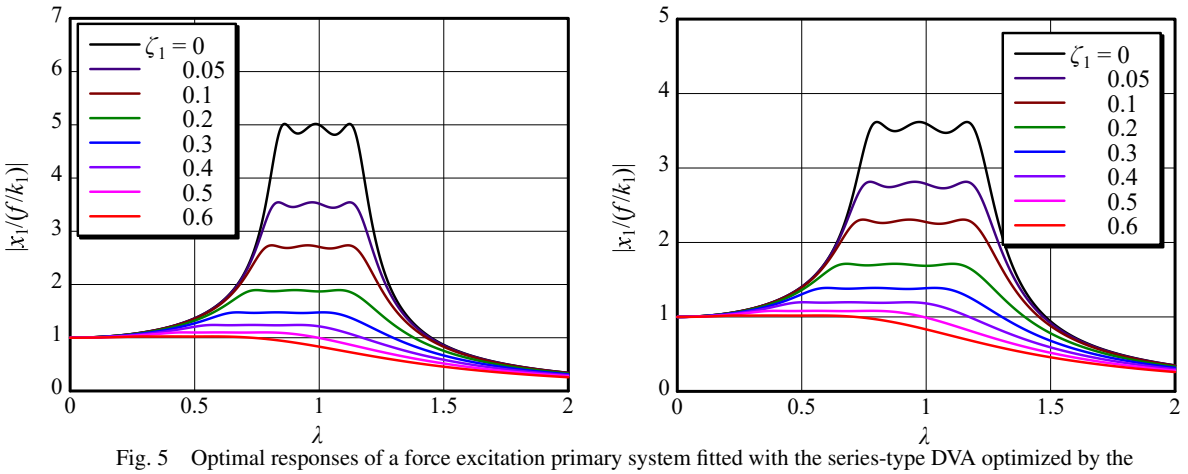

Fig. 5 Optimal responses of a force excitation primary system fitted with the series-type DVA optimized by the H_∞ criterion; (a) Mass ratio $\mu = 0.05$; (b) Mass ratio $\mu = 0.1$

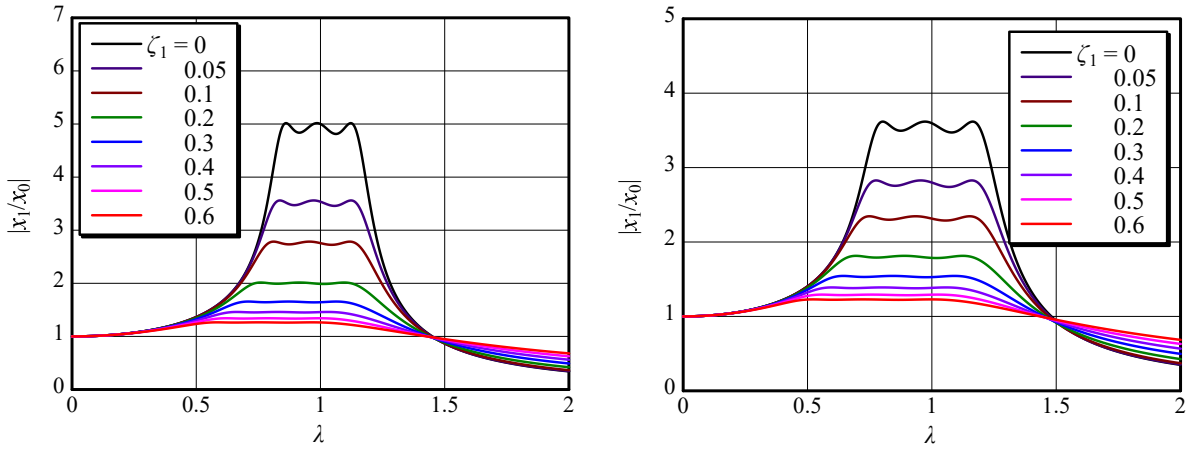

Fig. 6 Optimal responses of a motion excitation primary system fitted with the series-type DVA optimized by the H_∞ criterion; (a) Mass ratio $\mu = 0.05$; (b) Mass ratio $\mu = 0.1$

resonance points are equal:

$$\left.\begin{aligned} f_1 &= -r + r^3 + 4r\zeta_1^2 - 4r\zeta_1^4 + \ll 525 \text{ terms} \gg - 4r\zeta_3^4\mu^4\mu_B^4\nu^4\nu_B^4 = 0 \\ f_2 &= r^2 - r^3 - 2r^2\zeta_1^2 + 2r^3\zeta_2^2 + \ll 450 \text{ terms} \gg - 2\zeta_3^2\mu^3\mu_B^2\nu^4\nu_B^4 = 0 \\ f_3 &= 4r^4\zeta_3^2 - 4r^4\zeta_3^4 + 8r^4\zeta_3^2\nu_B - 8r^4\zeta_3^4\mu_B + \ll 167 \text{ terms} \gg + r^2\mu^2\mu_B^2\nu^4\nu_B^4 = 0. \end{aligned}\right\} \tag{18}$$

In the H_∞ optimization of the parallel-type double-mass DVA, the number of parameters to be optimized is six: μ_B, ν, ν_B, ζ_2, ζ_3, and r. Therefore, the number of formulas given in Eq. (18) is three fewer than the number needed to solve this optimization problem. The additional conditional expressions are derived from the following equation obtained from the fact that these simultaneous equations must have multiple roots:

$$\mathrm{d}r = \frac{\partial r}{\partial \mu_B}\mathrm{d}\mu_B + \frac{\partial r}{\partial \nu}\mathrm{d}\nu + \frac{\partial r}{\partial \nu_B}\mathrm{d}\nu_B + \frac{\partial r}{\partial \zeta_2}\mathrm{d}\zeta_2 + \frac{\partial r}{\partial \zeta_3}\mathrm{d}\zeta_3 = 0. \tag{19}$$

Because r is included in the functions f_1, f_2, and f_3, Eq. (19) can be rewritten as

$$\begin{bmatrix} \mathrm{d}r \\ \mathrm{d}r \\ \mathrm{d}r \end{bmatrix} = \begin{bmatrix} \dfrac{\partial r}{\partial f_1} & 0 & 0 \\ 0 & \dfrac{\partial r}{\partial f_2} & 0 \\ 0 & 0 & \dfrac{\partial r}{\partial f_3} \end{bmatrix} \begin{bmatrix} \dfrac{\partial f_1}{\partial \mu_B} & \dfrac{\partial f_1}{\partial \nu} & \dfrac{\partial f_1}{\partial \nu_B} & \dfrac{\partial f_1}{\partial \zeta_2} & \dfrac{\partial f_1}{\partial \zeta_3} \\ \dfrac{\partial f_2}{\partial \mu_B} & \dfrac{\partial f_2}{\partial \nu} & \dfrac{\partial f_2}{\partial \nu_B} & \dfrac{\partial f_2}{\partial \zeta_2} & \dfrac{\partial f_2}{\partial \zeta_3} \\ \dfrac{\partial f_3}{\partial \mu_B} & \dfrac{\partial f_3}{\partial \nu} & \dfrac{\partial f_3}{\partial \nu_B} & \dfrac{\partial f_3}{\partial \zeta_2} & \dfrac{\partial f_3}{\partial \zeta_3} \end{bmatrix} \begin{bmatrix} \mathrm{d}\mu_B \\ \mathrm{d}\nu \\ \mathrm{d}\nu_B \\ \mathrm{d}\zeta_2 \\ \mathrm{d}\zeta_3 \end{bmatrix} = \begin{bmatrix} 0 \\ 0 \\ 0 \end{bmatrix}. \tag{20}$$

Again, the 3×5 matrix in the equation is the Jacobian matrix. The condition of Eq. (20) equaling zero can be satisfied by setting the determinant of any arbitrary 3×3 submatrix extracted from this Jacobian matrix to zero. From this, the

[DOI: 10.1299/mej.19-00051]

remaining three equations needed to solve the optimization problem are obtained as follows:

$$\left.\begin{aligned} f_4 &= 128r^6\zeta_1\zeta_3\mu\mu_B\nu^2 - 256r^7\zeta_1\zeta_3^3\mu\mu_B\nu^2 + \ll 278674 \text{ terms} \gg + 128r^4\zeta_1\zeta_2\zeta_3^4\mu^7\mu_B^6\nu^{10}\nu_B^{11} = 0 \\ f_5 &= 128r^7\zeta_1\zeta_2^2\mu\nu_B - 128r^8\zeta_1\zeta_2^2\mu\nu_B + \ll 183411 \text{ terms} \gg + 512r^5\zeta_2\zeta_3^6\mu^8\mu_B^8\nu^9\nu_B^{11} = 0 \\ f_6 &= 128r^6\zeta_1\zeta_3^2\mu\mu_B\nu^2 - 256r^7\zeta_1\zeta_3^2\mu\mu_B\nu^2 + \ll 191969 \text{ terms} \gg + 256r^4\zeta_1\zeta_2\zeta_3^3\mu^7\mu_B^7\nu^{10}\nu_B^{11} = 0. \end{aligned}\right\} \quad (21)$$

When the values of μ and ζ_1 are known, the simultaneous algebraic equations given in Eqs. (18) and (21) can be solved using the Newton–Raphson method, which is included in *Mathematica*. The resulting solution consists of the five optimal parameter values $\mu_{B\text{opt}}$, ν_{opt}, $\nu_{B\text{opt}}$, $\zeta_{2\text{opt}}$, and $\zeta_{3\text{opt}}$ and the minimum value r_{min}.

4.2. H_∞ optimization for motion excitation system

Next, the DVA is optimized for the motion excitation system in Fig. 2(b). The equations of motion are

$$\left.\begin{aligned} &m_1\ddot{x}_1 + c_1(\dot{x}_1 - \dot{x}_0) + c_2(\dot{x}_1 - \dot{x}_2) + c_3(\dot{x}_1 - \dot{x}_3) + k_1(x_1 - x_0) + k_2(x_1 - x_2) + k_3(x_1 - x_3) = 0 \\ &m_2\ddot{x}_2 + c_2(\dot{x}_2 - \dot{x}_1) + k_2(x_2 - x_1) = 0, \quad m_3\ddot{x}_3 + c_3(\dot{x}_3 - \dot{x}_1) + k_3(x_3 - x_1) = 0. \end{aligned}\right\} \quad (22)$$

The simultaneous algebraic equations are given below

$$\left.\begin{aligned} f_1 &= -r + r^3 + 4r^3\zeta_1^2 - 4r^5\zeta_1^4 + \ll 543 \text{ terms} \gg - 4r\zeta_3^4\mu^4\mu_B^4\nu^4\nu_B^4 = 0 \\ f_2 &= r^2 - r^3 - 2r^4\zeta_1^2 + 2r^3\zeta_2^2 + \ll 448 \text{ terms} \gg - 2\zeta_3^2\mu^3\mu_B^2\nu^4\nu_B^4 = 0 \\ f_3 &= 4r^4\zeta_3^2 - 4r^4\zeta_3^4 + 8r^4\zeta_3^2\mu_B - 8r^4\zeta_3^4\mu_B + \ll 167 \text{ terms} \gg + r^2\mu^2\mu_B^2\nu^4\nu_B^4 = 0 \\ f_4 &= 128r^6\zeta_1\zeta_3^3\mu\mu_B\nu^2 - 256r^7\zeta_1\zeta_3^3\mu\mu_B\nu^2 + \ll 306049 \text{ terms} \gg + 128r^4\zeta_1\zeta_2\zeta_3^4\mu^7\mu_B^6\nu^{10}\nu_B^{11} = 0 \\ f_5 &= 128r^7\zeta_1\zeta_2^2\mu\nu_B - 128r^8\zeta_1\zeta_2^2\mu\nu_B + \ll 201986 \text{ terms} \gg + 512r^5\zeta_2\zeta_3^6\mu^8\mu_B^8\nu^9\nu_B^{11} = 0 \\ f_6 &= 128r^6\zeta_1\zeta_3^2\mu\mu_B\nu^2 - 256r^7\zeta_1\zeta_3^2\mu\mu_B\nu^2 + \ll 213924 \text{ terms} \gg + 256r^4\zeta_1\zeta_2\zeta_3^3\mu^7\mu_B^7\nu^{10}\nu_B^{11} = 0. \end{aligned}\right\} \quad (23)$$

These simultaneous equations can be solved numerically using the Newton–Raphson method.

4.3. Optimal values of design parameters for dynamic vibration absorber

Figure 7 shows the H_∞-optimal solution for the parallel-type double-mass DVA obtained by numerical analysis. The primary system damping ζ_1 is taken as the independent variable in these plots. As shown in this figure, as the damping ζ_1 of the primary system increases, the optimal parameters for the motion excitation system change less than do those for the force excitation system, with the exception of $\zeta_{3\text{opt}}$.

4.4. Minimized H_∞ performance index

In Fig. 8, panels (a) and (b) show the relationship between the height of the resonance points and the primary system damping for the parallel-type double-mass DVA optimized by the H_∞ criterion in the cases of force and motion excitation systems, respectively. A comparison of the results shown in Fig. 8 with the corresponding results for the series-type DVA shown in Fig. 4 reveals the similarity between the two cases; however, the response amplitude for the system with the parallel-type DVA takes on a large value when the primary system damping ζ_1 is less than 0.1. It has been demonstrated in a previous report (Asami, 2017) that the series-type DVA achieves better performance than the parallel-type DVA when there is no damping in the primary system, but the present results indicate that this also holds true even when the primary system includes a damping mechanism. The difference between the two types of DVAs becomes negligible when the primary system damping is greater than 0.1.

4.5. Frequency response for the primary system with a parallel-type dynamic vibration absorber optimized by the H_∞ criterion

Figure 9 shows the frequency response function for the system fitted with the parallel-type DVA optimized by the H_∞ criterion for the case of the force excitation system. A comparison of this frequency response function with that for the system having a series-type DVA shown in Fig. 5 confirms that at the same mass ratio, the resonance points in the system with the series-type DVA are lower than those in the system with the parallel-type DVA.

[DOI: 10.1299/mej.19-00051]

5. H_2 optimization of series-type dynamic vibration absorber

5.1. H_2 optimization for force excitation system

In the H_2 optimization of the DVA under force excitation, the objective is to minimize the following evaluation index:

$$I_a = \frac{1}{2\pi}\int_{-\infty}^{\infty}\left|\frac{x_1}{f/k_1}\right|^2 \mathrm{d}\lambda. \tag{24}$$

The minimum value of I_a is denoted $I_{a\min}$. In a previous study (Asami, 2019), the H_2-optimal solution was obtained

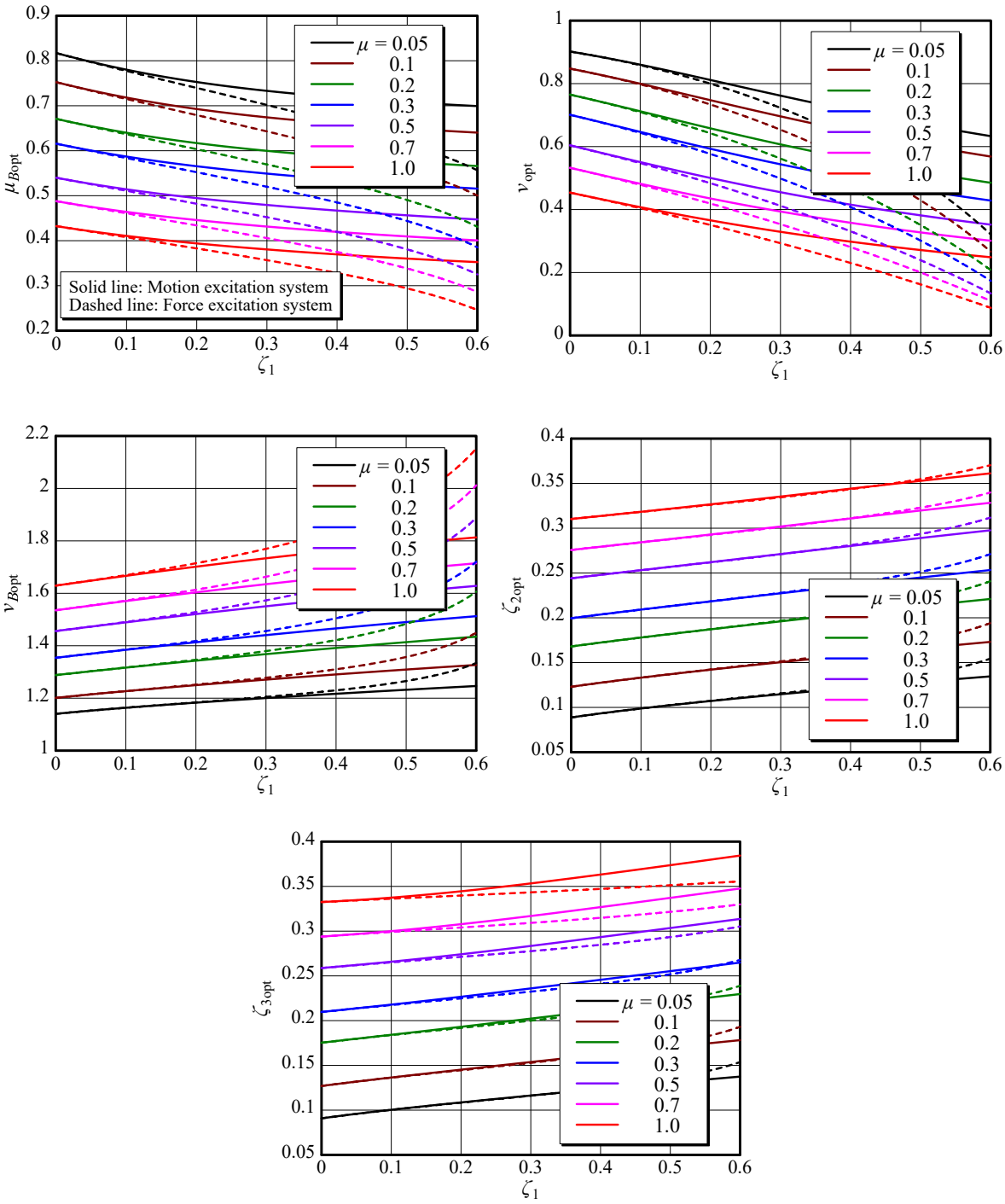

Fig. 7 H_∞-optimal solutions for the parallel-type DVA; (a) Optimal mass ratio $\mu_{B\mathrm{opt}}$; (b) Optimal tuning ratio ν_{opt}; (c) Optimal tuning ratio $\nu_{B\mathrm{opt}}$; (d) Optimal damping ratio $\zeta_{2\mathrm{opt}}$; (e) Optimal damping ratio $\zeta_{3\mathrm{opt}}$

[DOI: 10.1299/mej.19-00051]

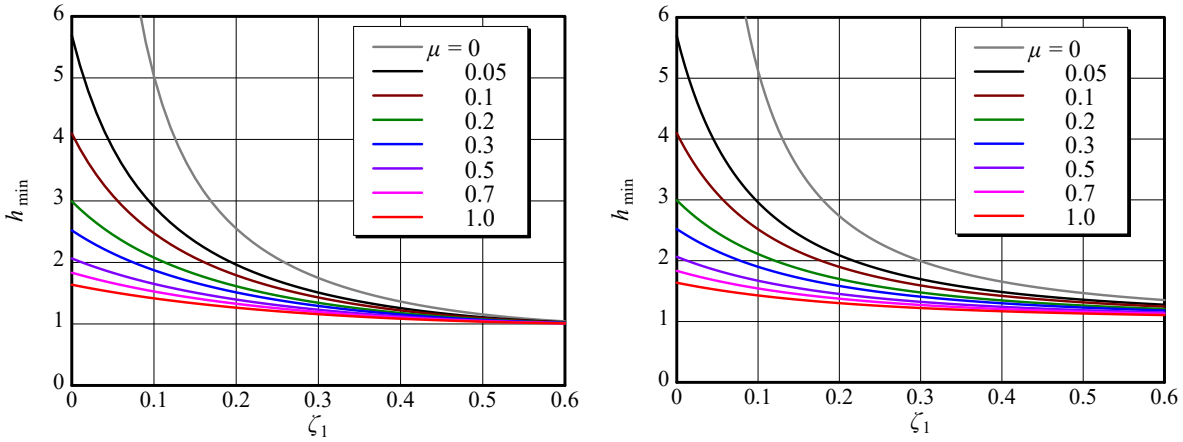

Fig. 8 Minimized response amplitude of primary systems fitted with the parallel-type DVA optimized by the H_∞ criterion; (a) Minimized amplitude $h_{\min}$ of the force excitation system; (b) Minimized amplitude $h_{\min}$ of the motion excitation system

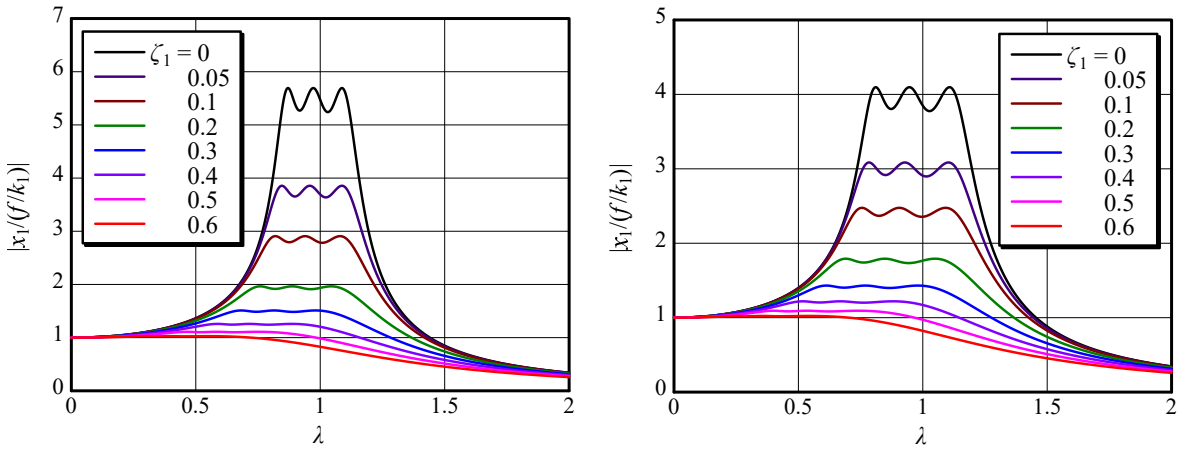

Fig. 9 Optimal responses of a force excitation primary system fitted with the parallel-type DVA optimized by the H_∞ criterion; (a) Mass ratio $\mu = 0.05$; (b) Mass ratio $\mu = 0.1$

algebraically as

$$\left.\begin{aligned} &\mu_{B\mathrm{opt}} = \mu + q_2^{1/3} + \mu^2 q_2^{-1/3},\quad \nu_{\mathrm{opt}} = \sqrt{1+\mu_{B\mathrm{opt}}},\quad \nu_{B\mathrm{opt}} = \frac{1}{1+\mu_{B\mathrm{opt}}},\quad \zeta_{2\mathrm{opt}} = 0,\quad \zeta_{3\mathrm{opt}} = \frac{\zeta_1\mu}{\nu_{\mathrm{opt}}(\mu_{B\mathrm{opt}} - 2\mu)} \\ &q_2 = \mu^2\left(2\zeta_1^2 - \mu + 2\zeta_1\sqrt{\zeta_1^2 - \mu}\right). \end{aligned}\right\} \quad (25)$$

This expression was obtained as a solution to a cubic algebraic equation solved by Cardano's method, in which an intermediate variable q_2 is permitted to be a complex number but all optima are calculated as positive real numbers.

5.2. H_2 optimization for motion excitation system

For the H_2 optimization of the motion excitation system shown in Fig. 1(b), the objective is to minimize the following evaluation index:

$$I_a = \frac{1}{2\pi}\int_{-\infty}^{\infty}\left|\frac{x_1}{x_0}\right|^2 \mathrm{d}\lambda. \quad (26)$$

In this case, only numerical solutions have been obtained (Asami et al., 2018).

5.3. Optimal values of design parameters for dynamic vibration absorber

Figure 10 shows the H_2-optimal solution of the DVA, which minimizes the area under the square of the compliance transfer function curve for the primary system. As is clear from these figures, in contrast to the H_∞-optimal solution, the primary system damping ζ_1 has less of an effect on the optimized parameter values in the force excitation system than on those in the motion excitation system. One point that sets the H_2-optimal solution apart from the H_∞-optimal solution described above is that the value of the natural angular frequency ratio ν_{opt} monotonically increases with increasing ζ_1.

[DOI: 10.1299/mej.19-00051]

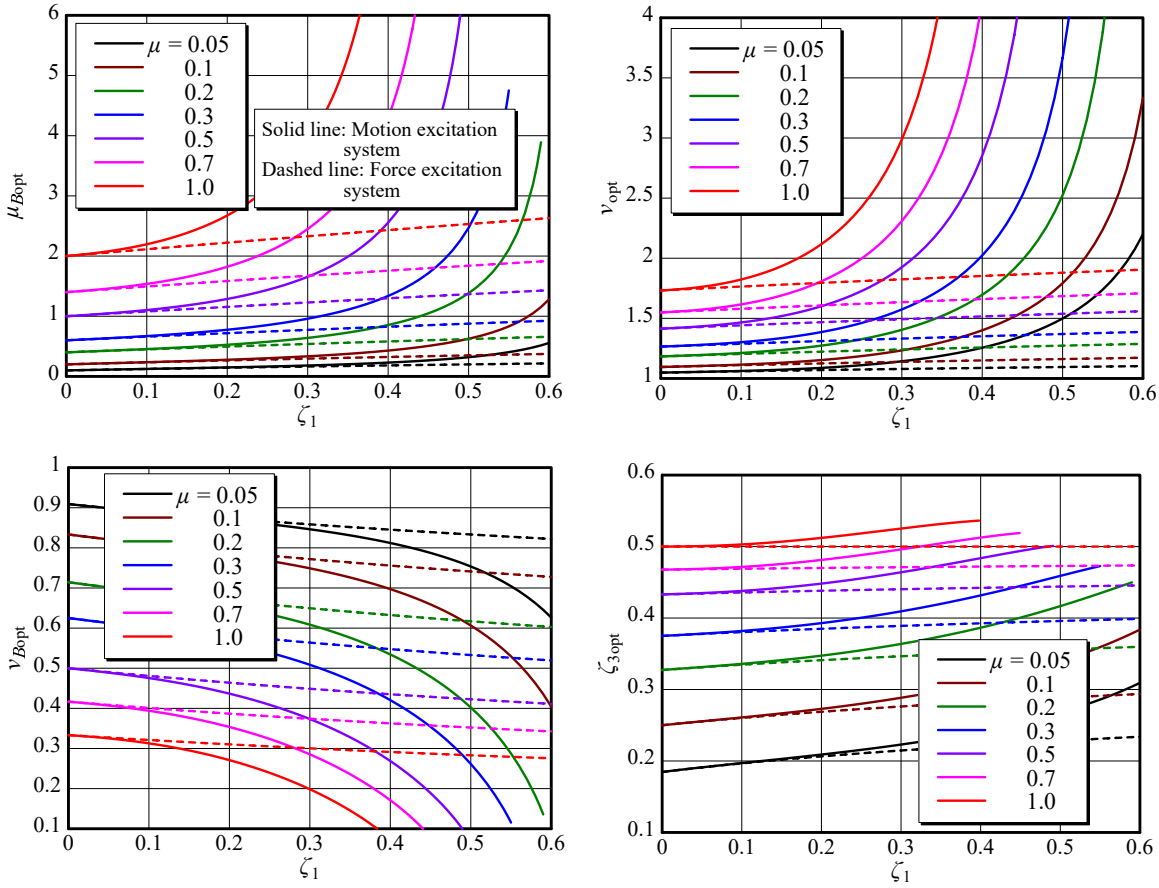

Fig. 10 H_2-optimal solutions for the series-type DVA; (a) Optimal mass ratio $\mu_{B\mathrm{opt}}$; (b) Optimal tuning ratio ν_{opt}; (c) Optimal tuning ratio $\nu_{B\mathrm{opt}}$; (d) Optimal damping ratio $\zeta_{3\mathrm{opt}}$

The solid lines do not span the entire range of ζ_1 values in Fig. 10, which means that the motion excitation has no solution for the ζ_1 values beyond the endpoints of the lines.

5.4. Minimized H_2 performance index

Figure 11 shows the value of the area under the square of the compliance transfer function curve for the primary system fitted with the series-type DVA optimized by the H_2 criterion. The curve for $\mu = 0$ shown in gray represents the case when the primary system is not fitted with a DVA, and the effect of the DVA can be seen with this curve considered as a point of reference.

5.5. Frequency response of the primary system with a series-type dynamic vibration absorber optimized by the H_2 criterion

Figure 12 shows the frequency response function for the force excitation system with the series-type DVA optimized by the H_2 criterion. As shown in this figure, when the DVA optimized by the H_2 criterion is attached to the primary system, the three resonance amplitudes for the primary system always decrease in the order of the 1st-, 2nd-, and 3rd-order peaks. Inevitably, the maximum resonance point is higher than that achieved by H_∞ optimization.

6. H_2 optimization of parallel-type dynamic vibration absorber

6.1. H_2 optimization for force excitation system

The definite integral shown in Eq. (24) was solved by the residue theorem (Kreyszig, 1999), and the result can be expressed in a fractional form as follows:

$$\left.\begin{aligned} I_a &= \frac{1}{2\pi}\int_{-\infty}^{\infty}\left|\frac{x_1}{f/k_1}\right|^2 \mathrm{d}\lambda = \frac{I_{a\mathrm{Num}}}{I_{a\mathrm{Den}}} \\ I_{a\mathrm{Num}} &= \zeta_2\zeta_3 + 3\zeta_2\zeta_3\mu_B + 3\zeta_2\zeta_3\mu_B^2 + \ll 3024\ \text{terms} \gg + \zeta_2\zeta_3\mu^4\mu_B^3\nu^8\nu_B^8 \\ I_{a\mathrm{Den}} &= 4(\zeta_1\zeta_2\zeta_3 + 3\zeta_1\zeta_2\zeta_3\mu_B + 3\zeta_1\zeta_2\zeta_3\mu_B^2 + \ll 3276\ \text{terms} \gg + \zeta_1\zeta_2\zeta_3\mu^4\mu_B^3\nu^8\nu_B^8). \end{aligned}\right\} \quad (27)$$

[DOI: 10.1299/mej.19-00051]

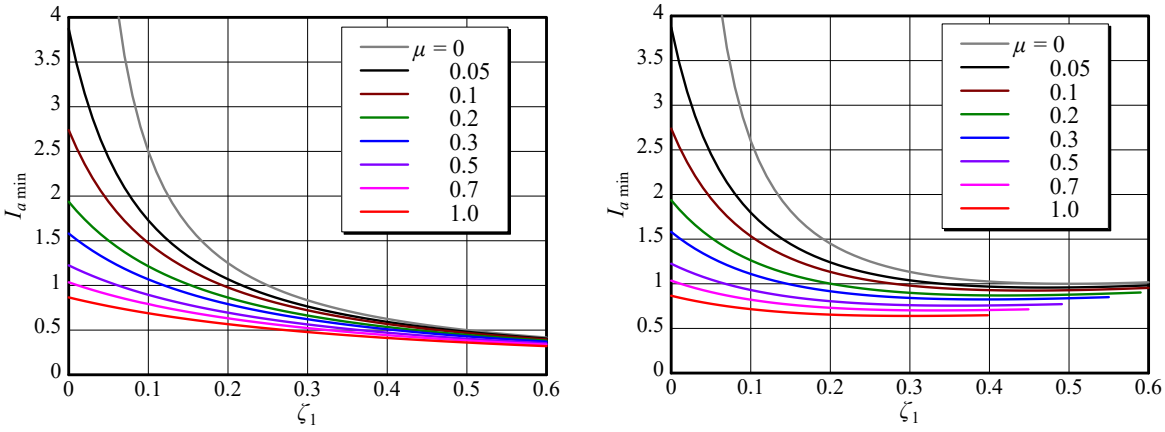

Fig. 11 Minimized evaluation index of primary systems fitted with the series-type DVA optimized by the H_2 criterion; (a) Evaluation index $I_{a\min}$ for the force excitation system; (b) Evaluation index $I_{a\min}$ for the motion excitation system

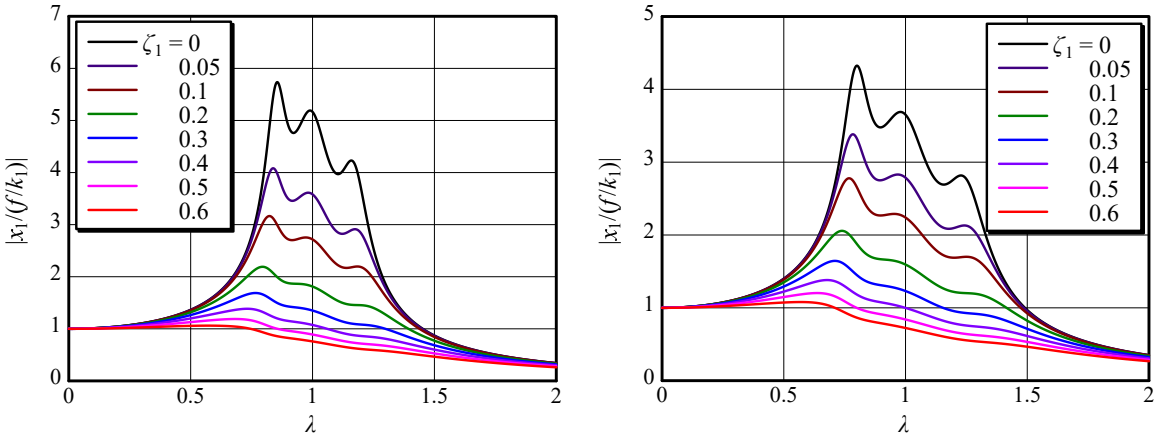

Fig. 12 Optimal responses of a force excitation primary system fitted with the series-type DVA optimized by the H_2 criterion; (a) Mass ratio $\mu = 0.05$; (b) Mass ratio $\mu = 0.1$

When this equation is partially differentiated with respect to each of the five parameters to be optimized and the sum of the partial differentials is set to zero, the following simultaneous algebraic equations are obtained:

$$\left.\begin{aligned}
f_1 &= \zeta_2^3\zeta_3^2 + 2\zeta_2^3\zeta_3^2\mu_B + 6\zeta_2^3\zeta_3^2\mu_B^2 + \ll 65216\ \text{terms} \gg + \zeta_1\zeta_2^2\zeta_3^2\mu^6\mu_B^4\nu^{13}\nu_B^{16} = 0\\
f_2 &= -\zeta_2^3\zeta_3^2 - 5\zeta_2^3\zeta_3^2\mu_B - 10\zeta_2^3\zeta_3^2\mu_B^2 + \ll 83146\ \text{terms} \gg + 2\zeta_1\zeta_2^2\zeta_3^2\mu^6\mu_B^5\nu^{13}\nu_B^{16} = 0\\
f_3 &= -\zeta_2^3\zeta_3^2 - 5\zeta_2^3\zeta_3^2\mu_B - 10\zeta_2^3\zeta_3^2\mu_B^2 + \ll 61169\ \text{terms} \gg + 2\zeta_1\zeta_2^2\zeta_3^2\mu^6\mu_B^5\nu^{13}\nu_B^{13} = 0\\
f_4 &= -\zeta_2^2\zeta_3^2 - 5\zeta_2^2\zeta_3^2\mu_B - 10\zeta_2^2\zeta_3^2\mu_B^2 + \ll 55055\ \text{terms} \gg - \zeta_2^2\zeta_3^2\mu^6\mu_B^5\nu^{12}\nu_B^{16} = 0\\
f_5 &= -\zeta_2^2\zeta_3^2 - 5\zeta_2^2\zeta_3^2\mu_B - 10\zeta_2^2\zeta_3^2\mu_B^2 + \ll 55038\ \text{terms} \gg - \zeta_2^2\zeta_3^2\mu^6\mu_B^5\nu^{12}\nu_B^{16} = 0.
\end{aligned}\right\} \tag{28}$$

In H_2 optimization, the number of simultaneous equations is one fewer than that in H_∞ optimization. It is impossible to solve these equations algebraically, but they can be solved numerically by the Newton–Raphson method starting from a suitable initial value.

6.2. H_2 optimization for motion excitation system

Subsequently, optimization of the DVA attached to the motion excitation system shown in Fig. 2(b) was performed. As in the force excitation system, the evaluation index I_a for the H_2 criterion can be calculated as follows:

$$\left.\begin{aligned}
I_a &= \frac{1}{2\pi}\int_{-\infty}^{\infty}\left|\frac{x_1}{x_0}\right|^2 \mathrm{d}\lambda = \frac{I_{a\mathrm{Num}}}{I_{a\mathrm{Den}}}\\
I_{a\mathrm{Num}} &= \zeta_2\zeta_3 + 4\zeta_1^2\zeta_2\zeta_3 + 3\zeta_2\zeta_3\mu_B + \ll 4596\ \text{terms} \gg + \zeta_2\zeta_3\mu^4\mu_B^3\nu^8\nu_B^8\\
I_{a\mathrm{Den}} &= 4(\zeta_1\zeta_2\zeta_3 + 3\zeta_1\zeta_2\zeta_3\mu_B + 3\zeta_1\zeta_2\zeta_3\mu_B^2 + \ll 3276\ \text{terms} \gg + \zeta_1\zeta_2\zeta_3\mu^4\mu_B^3\nu^8\nu_B^8).
\end{aligned}\right\} \tag{29}$$

[DOI: 10.1299/mej.19-00051]

Only the numerator $I_{a\mathrm{Num}}$ of the evaluation index sets this equation apart from the corresponding equation for the force excitation system. In the same way as above, the following simultaneous equations can be obtained:

$$\left.\begin{aligned}
f_1 &= \zeta_2^3\zeta_3^2 + 4\zeta_1^2\zeta_2^3\zeta_3^2 + 4\zeta_2^3\zeta_3^2\mu_B^2 + \ll 119177 \text{ terms} \gg - 8\zeta_1^4\zeta_2\zeta_3^2\mu^5\mu_B^3\nu^{14}\nu_B^{16} = 0\\
f_2 &= -\zeta_2^3\zeta_3^2 - 4\zeta_1^2\zeta_2^3\zeta_3^2 - 5\zeta_2^3\zeta_3^2\mu_B + \ll 158994 \text{ terms} \gg - 4\zeta_1^4\zeta_2\zeta_3^2\mu^5\mu_B^4\nu^{14}\nu_B^{16} = 0\\
f_3 &= -\zeta_2^3\zeta_3^2 - 4\zeta_1^2\zeta_2^2\zeta_3^3 - 5\zeta_2^2\zeta_3^3\mu_B + \ll 114438 \text{ terms} \gg - 4\zeta_1^4\zeta_2^2\zeta_3\mu^6\mu_B^5\nu^{14}\nu_B^{14} = 0\\
f_4 &= -\zeta_2^2\zeta_3^2 - 4\zeta_1^2\zeta_2^2\zeta_3^2 - 5\zeta_2^2\zeta_3^2\mu_B + \ll 95009 \text{ terms} \gg - 4\zeta_1^4\zeta_3^2\mu^5\mu_B^4\nu^{14}\nu_B^{16} = 0\\
f_5 &= -\zeta_2^2\zeta_3^2 - 4\zeta_1^2\zeta_2^2\zeta_3^2 - 5\zeta_2^2\zeta_3^2\mu_B + \ll 95009 \text{ terms} \gg - 4\zeta_1^4\zeta_2^2\mu^6\mu_B^5\nu^{14}\nu_B^{14} = 0.
\end{aligned}\right\} \tag{30}$$

These simultaneous equations can be solved numerically by the Newton–Raphson method.

6.3. Optimal values of design parameters of dynamic vibration absorber

The H_2-optimal solution for the DVA obtained by numerical analysis is shown in Fig. 13. The solution at $\zeta_1 = 0$ is consistent with that for the undamped primary system reported in a previous paper (Asami et al., 2018). Although the optimal solution for the force excitation system changes little with increasing primary system damping, that for the motion excitation system begins to change significantly from approximately $\zeta_1 = 0.1$. As shown in Fig. 13(a), as ζ_1 increases, $\mu_{B\mathrm{opt}}$ reaches a maximum and then suddenly decreases. In contrast, $\nu_{B\mathrm{opt}}$ and $\zeta_{2\mathrm{opt}}$ suddenly increase after progressing through local maximum and minimum values, as shown respectively in panels (c) and (d) of Fig. 13.

Of particular interest among the optimized design parameters is the optimal mass ratio μ_B shown in Fig. 13(a). As described in Section 2, because the larger DVA of the two is defined as DVA-A, the value of μ_B is initially less than one. As the primary system damping ζ_1 increases, this optimal mass ratio reaches a region where it suddenly increases and reaches its maximum value of approximately two. The relationship between the sizes of the two DVAs is reversed near this maximum value. Among the three optimization criteria, H_2 optimization achieves the smallest damping ratio for the DVA. However, an unexpected result was that the optimal damping ratio $\zeta_{3\mathrm{opt}}$ for DVA-B takes a large value.

6.4. Minimized H_2 performance index

In Fig. 14, panels (a) and (b) show the values of the minimized evaluation index $I_{a\mathrm{min}}$ for the force and motion excitation systems, respectively. In the force excitation system, $I_{a\mathrm{min}}$ decreases monotonically as the primary system damping ζ_1 increases because the primary system is mounted on an immovable foundation. In contrast, for the motion excitation system, $I_{a\mathrm{min}}$ takes a minimum value at a certain value of ζ_1 and then begins to increase. In these figures, the curve for $\mu = 0$ shown in gray is the value of the evaluation index for the vibratory system with no DVA attached.

6.5. Frequency response of the primary system with a parallel-type dynamic vibration absorber optimized by the H_2 criterion

Figure 15 shows the frequency response function for the primary system in the force excitation system shown in Fig. 2(a). The two panels of Fig. 15 show the response of the primary system when DVAs of different sizes are attached. A comparison of these results with those shown in Fig. 12, which represents the response of a system with the series-type DVA, reveals that the system with the parallel-type DVA has higher resonance points.

7. Stability maximization of series-type dynamic vibration absorber

In the optimization by the stability criterion, the DVA is designed to maximize the stability of the system, defined by the following formula (Asami et al., 2018):

$$\Lambda = -\max(\mathrm{Re}[s_i]). \tag{31}$$

The following algebraic exact solution has already been obtained for the series-type DVA (Asami, 2019):

$$\left.\begin{aligned}
&\mu_{B\mathrm{opt}} = 4\zeta_1^2 + 5\mu + 3q_3^{1/3} + 3\mu(8\zeta_1^2+\mu)q_3^{-1/3},\quad \nu_{\mathrm{opt}} = \sqrt{1+\mu_{B\mathrm{opt}}},\quad \nu_{B\mathrm{opt}} = \frac{1}{1+\mu_{B\mathrm{opt}}}\\
&\zeta_{2\mathrm{opt}} = 0,\quad \zeta_{3\mathrm{opt}} = \frac{\zeta_1 + \sqrt{3(\mu-\zeta_1^2+\mu_{B\mathrm{opt}})}}{2\nu_{\mathrm{opt}}},\quad \Lambda_{\max} = \frac{3\zeta_1 + \sqrt{3(\mu-\zeta_1^2+\mu_{B\mathrm{opt}})}}{6}\\
&q_3 = \mu\left[8\zeta_1^4 + 8\zeta_1(\zeta_1^2-\mu)^{3/2} + 20\zeta_1^2\mu - \mu^2\right].
\end{aligned}\right\} \tag{32}$$

[DOI: 10.1299/mej.19-00051]

8. Stability maximization of parallel-type dynamic vibration absorber

8.1. Optimization procedure

The characteristic equation for the system shown in Fig. 2 is

$$s^6 + a_1 s^5 + a_2 s^4 + a_3 s^3 + a_4 s^2 + a_5 s + a_6 = 0, \tag{33}$$

$$\left.\begin{aligned} a_1 &= 2\zeta_1 + 2\zeta_2\left(1 + \frac{\mu}{1+\mu_B}\right)\nu + 2\zeta_3\left(1 + \frac{\mu\mu_B}{1+\mu_B}\right)\nu\nu_B \\ a_2 &= 1 + \left(1 + \frac{\mu}{1+\mu_B}\right)\nu^2 + \left(1 + \frac{\mu\mu_B}{1+\mu_B}\right)\nu^2\nu_B^2 + 4\zeta_1\zeta_2\nu + 4\zeta_1\zeta_3\nu\nu_B + 4\zeta_2\zeta_3(1+\mu)\nu^2\nu_B \end{aligned}\right\} \tag{34}$$

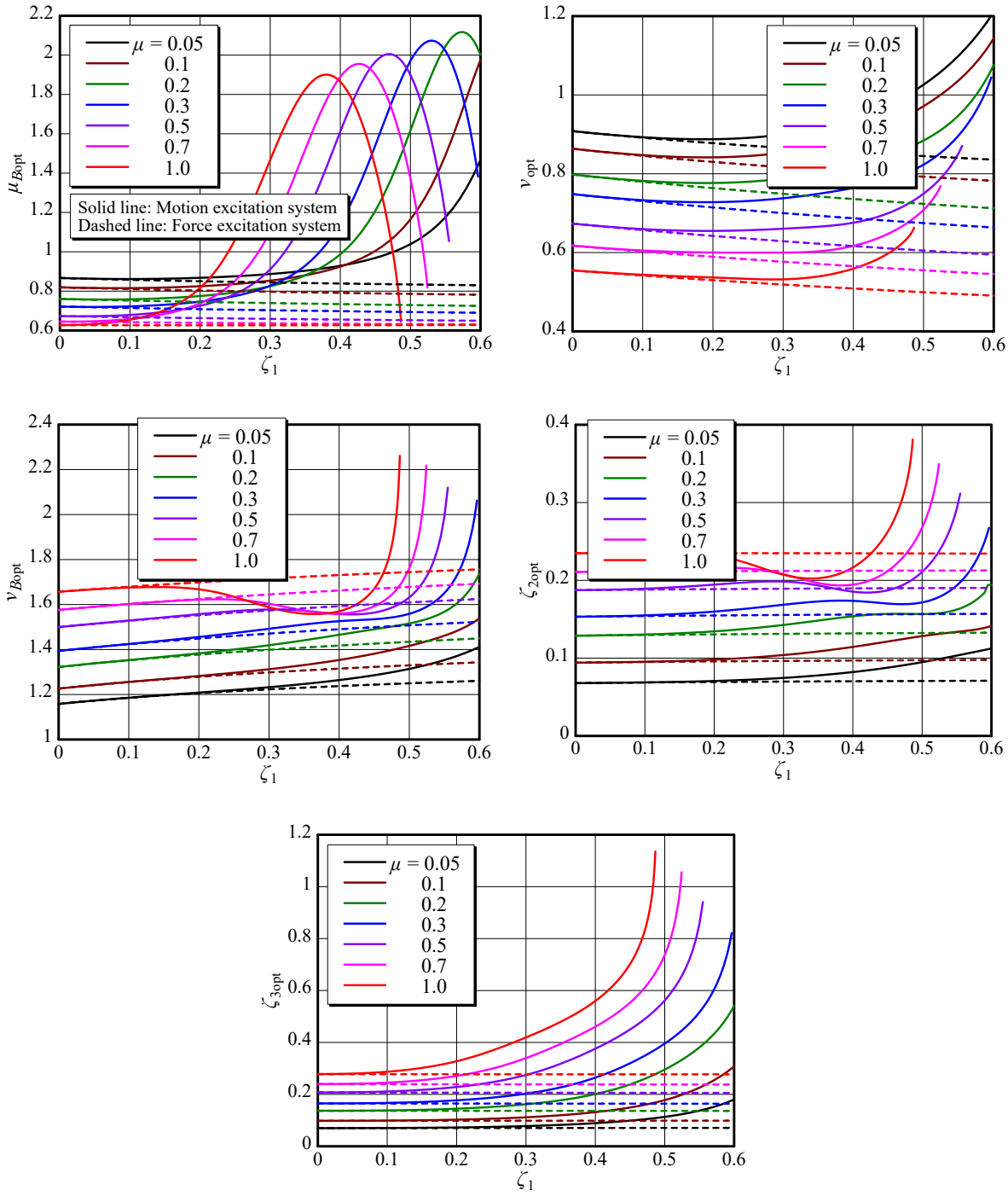

Fig. 13 H_2-optimal solutions for the parallel-type DVA; (a) Optimal mass ratio $\mu_{B\mathrm{opt}}$; (b) Optimal tuning ratio ν_{opt}; (c) Optimal tuning ratio $\nu_{B\mathrm{opt}}$; (d) Optimal damping ratio $\zeta_{2\mathrm{opt}}$; (e) Optimal damping ratio $\zeta_{3\mathrm{opt}}$

[DOI: 10.1299/mej.19-00051]

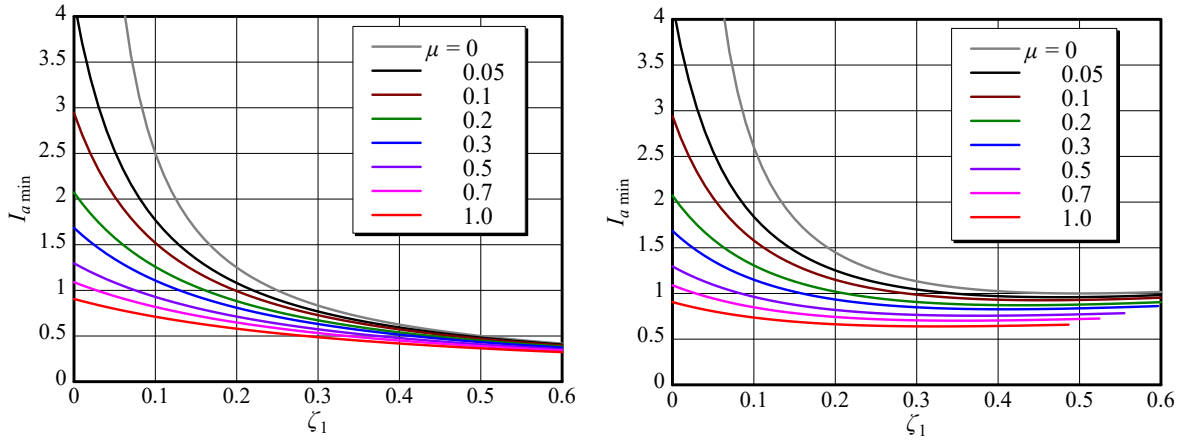

Fig. 14 Minimized evaluation index for primary systems fitted with the parallel-type DVA optimized by the H_2 criterion; (a) Evaluation index $I_{a\min}$ for the force excitation system; (b) Evaluation index $I_{a\min}$ for the motion excitation system

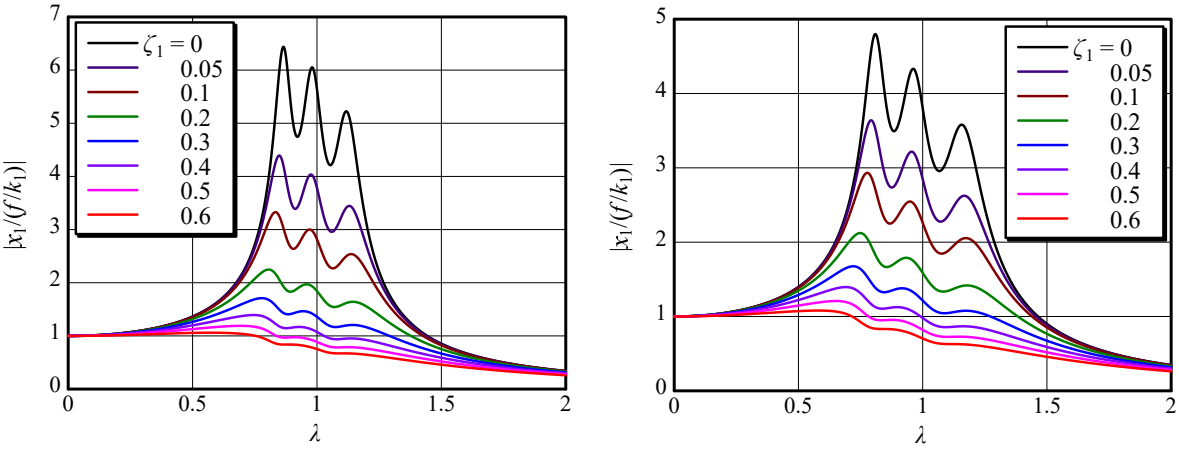

Fig. 15 Optimal responses of a force excitation primary system fitted with the parallel-type DVA optimized by the H_2 criterion; (a) Mass ratio $\mu = 0.05$; (b) Mass ratio $\mu = 0.1$

$$\left.\begin{aligned} a_3 &= 2\nu[\zeta_1\nu(1+\nu_B^2) + \zeta_2(1+\nu^2\nu_B^2 + \mu\nu^2\nu_B^2) + \zeta_3(1+\nu^2+\mu\nu^2)\nu_B + 4\zeta_1\zeta_2\zeta_3\nu\nu_B] \\ a_4 &= \nu^2[1 + (1+\nu^2+\mu\nu^2)\nu_B^2 + 4\zeta_1\zeta_2\nu\nu_B^2 + 4\zeta_1\zeta_3\nu\nu_B + 4\zeta_2\zeta_3\nu_B] \\ a_5 &= 2\nu^3\nu_B(\zeta_1\nu\nu_B + \zeta_2\nu_B + \zeta_3), \quad a_6 = \nu^4\nu_B^2. \end{aligned}\right\} \tag{35}$$

From previous research (Asami et al., 2018), it is known that when the stability Λ of a three-degree-of-freedom system is maximized, the characteristic equation has a triple root. In this case, Eqs. (34) and (35) can be factored as

$$D(s) = [s - (x_r + iy_r)]^3[s - (x_r - iy_r)]^3, \tag{36}$$

where (x_r, y_r) are the coordinates of the complex conjugate root in the complex plane. Expanding Eq. (36), rearranging it by the power of s, and comparing the coefficients with those in Eqs. (34) and (35) yields the following six identities:

$$\left.\begin{aligned} f_1 &= 3x_r(1+\mu_B) + \zeta_1(1+\mu_B) + \zeta_2(1+\mu+\mu_B)\nu + \zeta_3[1+(1+\mu)\mu_B]\nu\nu_B = 0 \\ f_2 &= (1 - 15x_r^2 - 3y_r^2)(1+\mu_B) + \nu^2\{1+\mu+\mu_B + [1+(1+\mu)\mu_B]\nu_B^2\} + 4\zeta_1\zeta_2(1+\mu_B)\nu + 4\zeta_1\zeta_3(1+\mu_B)\nu\nu_B \\ &\quad + 4\zeta_2\zeta_3(1+\mu)(1+\mu_B)\nu^2\nu_B = 0 \\ f_3 &= 2x_r(5x_r^2 + 3y_r^2) + \zeta_1\nu^2(1+\nu_B^2) + \zeta_2\nu[1+(1+\mu)\nu^2\nu_B^2] + \zeta_3\nu[1+(1+\mu)\nu^2]\nu_B + 4\zeta_1\zeta_2\zeta_3\nu^2\nu_B = 0 \\ f_4 &= -3(x_r^2+y_r^2)(5x_r^2+y_r^2) + \nu^2[1+\nu_B^2+(1+\mu)\nu^2\nu_B^2] + 4\zeta_1\zeta_2\nu^3\nu_B^2 + 4\zeta_1\zeta_3\nu^3\nu_B + 4\zeta_2\zeta_3\nu^2\nu_B = 0 \\ f_5 &= 3x_r(x_r^2+y_r^2)^2 + \zeta_1\nu^4\nu_B^2 + \zeta_2\nu^3\nu_B^2 + \zeta_3\nu^3\nu_B = 0, \quad f_6 = -(x_r^2+y_r^2)^3 + \nu^4\nu_B^2 = 0. \end{aligned}\right\} \tag{37}$$

Equation (37) is not a complete system of simultaneous equations, but it contains equations that can be solved separately.

[DOI: 10.1299/mej.19-00051]

From the first and sixth equations, the following solutions are obtained:

$$\zeta_{3\mathrm{opt}} = \frac{-3x_r(1+\mu_B) - \zeta_1(1+\mu_B) - \zeta_2(1+\mu+\mu_B)\nu}{[1+(1+\mu)\mu_B]\nu\nu_B} \tag{38}$$

and

$$\nu_{B\mathrm{opt}} = (x_r^2 + y_r^2)^{3/2}/\nu^2. \tag{39}$$

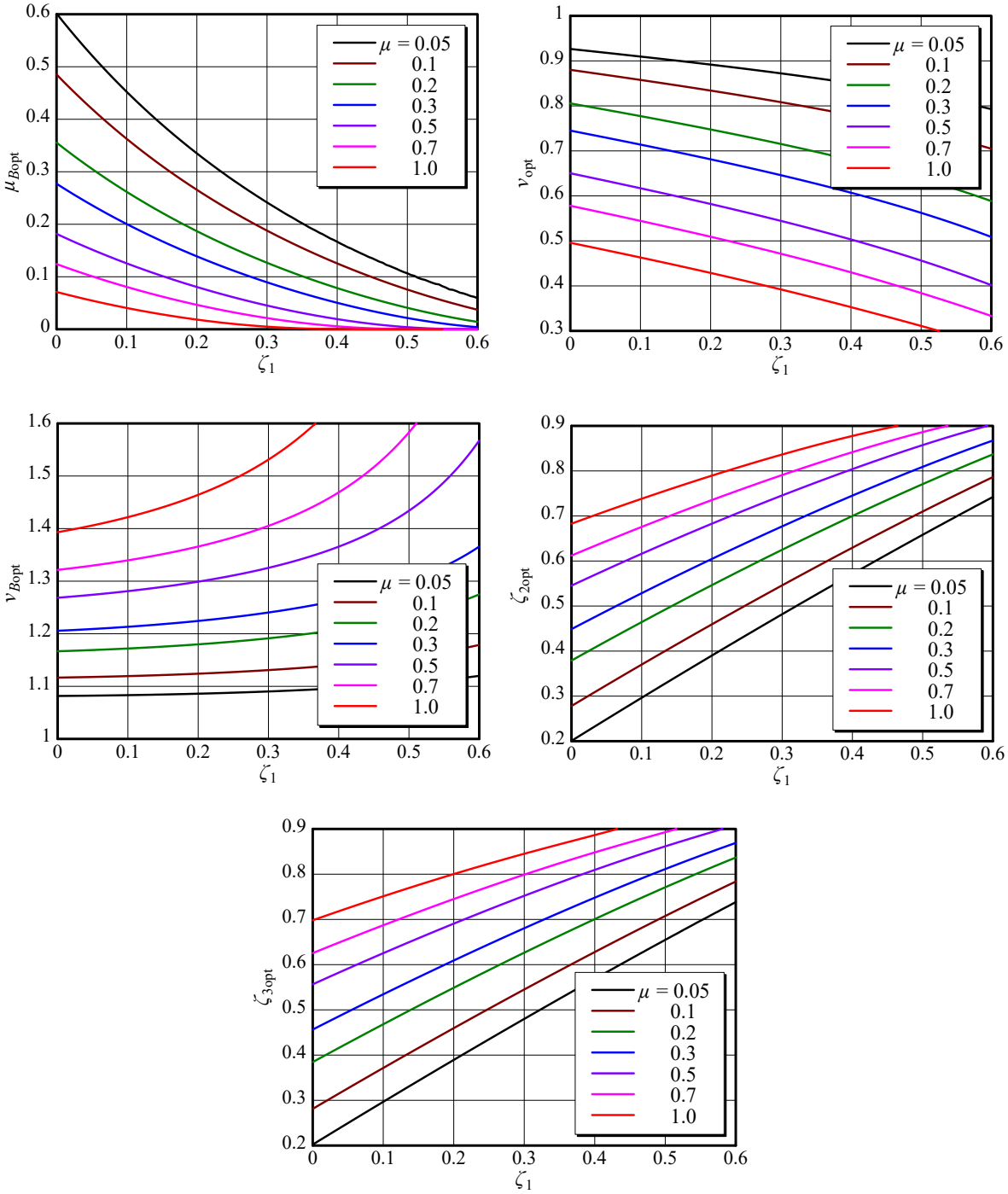

Fig. 16 Optimal solutions based on the stability criterion for the parallel-type DVA; (a) Optimal mass ratio $\mu_{B\mathrm{opt}}$; (b) Optimal tuning ratio ν_{opt}; (c) Optimal tuning ratio $\nu_{B\mathrm{opt}}$; (d) Optimal damping ratio $\zeta_{2\mathrm{opt}}$; (e) Optimal damping ratio $\zeta_{3\mathrm{opt}}$

[DOI: 10.1299/mej.19-00051]

These can be substituted into the fifth equation of Eq. (37) to obtain

$$\left.\begin{aligned} &\mu_{B\mathrm{opt}} = \mu_{B\mathrm{Num}}/\mu_{B\mathrm{Den}} \\ &\mu_{B\mathrm{Num}} = 3x_r[\nu^2 - (x_r^2 + y_r^2)^2]\nu - (x_r^2 + y_r^2)^3(\zeta_1\nu + \zeta_2) + \nu^3[\zeta_1 + (1+\mu)\zeta_2\nu] \\ &\mu_{B\mathrm{Den}} = 3x_r(x_r^2 + y_r^2)^2(1+\mu)\nu - 3x_r\nu^3 + (x_r^2 + y_r^2)^3(\zeta_1\nu + \zeta_2)(1+\mu) - \nu^3(\zeta_1 + \zeta_2\nu). \end{aligned}\right\} \quad (40)$$

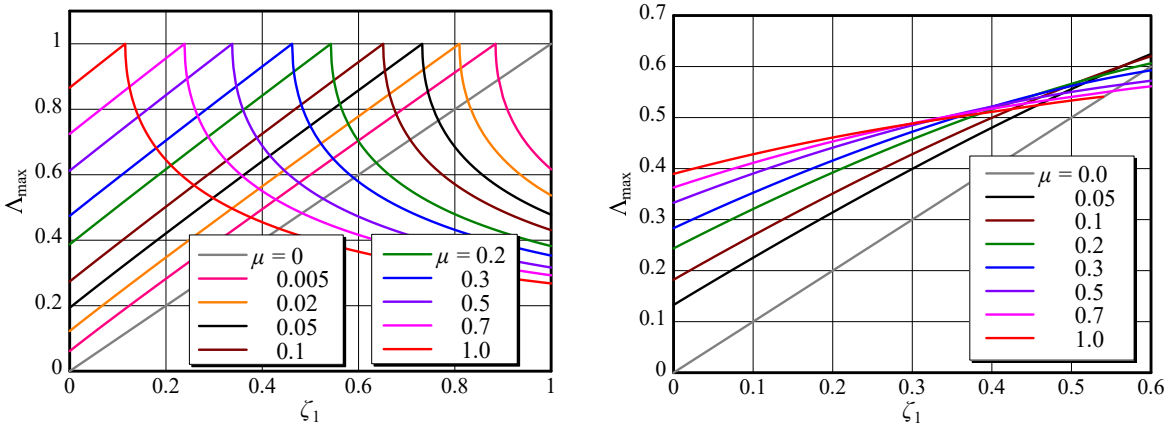

Fig. 17 Maximized stabilities of vibratory systems fitted with double-mass DVAs; (a) Maximized stability $\Lambda_{\max}$ for the series-type DVA; (b) Maximized stability $\Lambda_{\max}$ for the parallel-type DVA

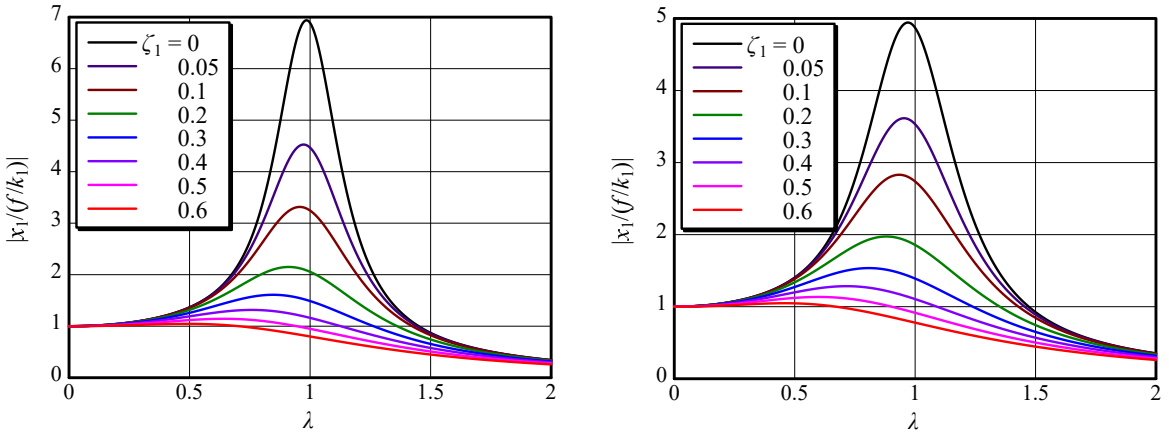

Fig. 18 Optimal responses of a force excitation primary system fitted with the series-type DVA optimized by the stability criterion; (a) Mass ratio $\mu = 0.05$; (b) Mass ratio $\mu = 0.1$

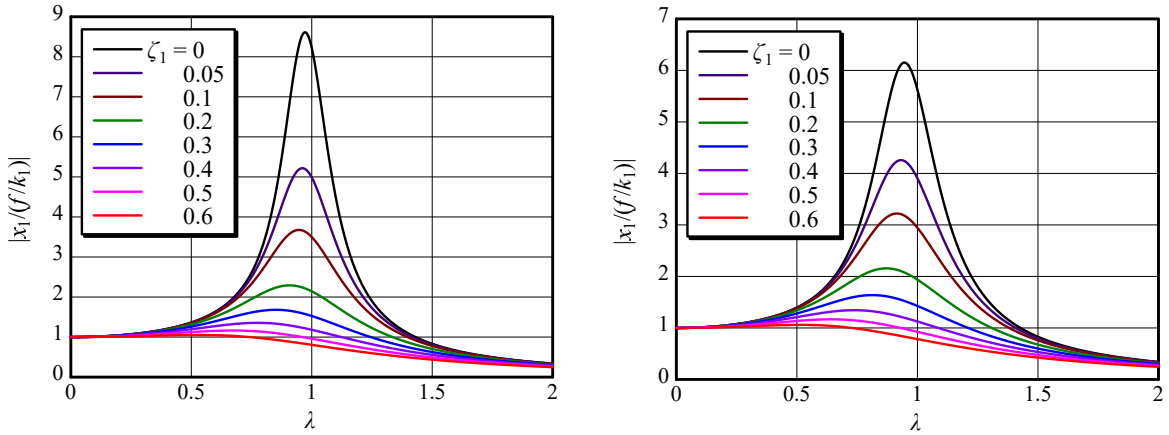

Fig. 19 Optimal responses of a force excitation primary system fitted with the parallel-type DVA optimized by the stability criterion; (a) Mass ratio $\mu = 0.05$; (b) Mass ratio $\mu = 0.1$

[DOI: 10.1299/mej.19-00051]

Furthermore, the following solution can be derived by substituting the fourth equation into the third equation:

$$\left.\begin{aligned}
&\zeta_{2\mathrm{opt}} = \nu\zeta_{2\mathrm{Num}}/\zeta_{2\mathrm{Den}} \\
&\zeta_{2\mathrm{Num}} = 2x_r(5x_r^2+3y_r^2)^2\nu^2 - 3x_r(x_r^2+y_r^2)^2(1+\nu^2+\mu\nu^2) - (x_r^2+y_r^2)^3\zeta_1(1+2\nu^2+2\mu\nu^2) \\
&\quad + 3(x_r^2+y_r^2)(5x_r^2+y_r^2)\zeta_1\nu^2 + 12x_r^2(x_r^2+y_r^2)^2\zeta_1^2\nu^2 + 4(x_r^2+y_r^2)^3\zeta_1^3\nu^2 \\
&\zeta_{2\mathrm{Den}} = (x_r^2+y_r^2)^3 - \nu^4.
\end{aligned}\right\} \tag{41}$$

In the stability optimization of the parallel-type double-mass DVA, the number of parameters to be optimized is five. In addition to this, it is necessary to find the coordinates (x_r, y_r) of the pole in the stability maximization criterion, meaning there are a total of seven unknowns. However, the number of equations given in Eq. (37) is only six, necessitating the derivation of another equation. At this stage, the remaining equations in Eq. (37) can be expressed as follows:

$$\left.\begin{aligned}
&f_2 = x_r^{25} + 36x_r^{23}y_r^2 + 198x_r^{21}y_r^4 + \ll 8590\ \text{terms} \gg + 3x_r\nu^{16} + \zeta_1\nu^{16} = 0 \\
&f_4 = x_r^{18} + 9x_r^{16}y_r^2 + 36x_r^{14}y_r^4 + \ll 777\ \text{terms} \gg + y_r^6\mu\nu^{10} + \nu^{12} = 0.
\end{aligned}\right\} \tag{42}$$

These two simultaneous equations contain three unknowns, x_r, y_r, and ν. Therefore, another equation is needed to determine these unknowns. The equation to be added is the condition that the total derivative with respect to y_r and ν of the x coordinates x_r of the characteristic roots should be zero; that is,

$$\mathrm{d}x_r = \frac{\partial x_r}{\partial y_r}\mathrm{d}y_r + \frac{\partial x_r}{\partial \nu}\mathrm{d}\nu = 0. \tag{43}$$

Because r is included in the functions f_2 and f_4, Eq. (43) can be rewritten as

$$\begin{bmatrix} \mathrm{d}x_r \\ \mathrm{d}x_r \end{bmatrix} = \begin{bmatrix} \dfrac{\partial x_r}{\partial f_2} & 0 \\ 0 & \dfrac{\partial x_r}{\partial f_4} \end{bmatrix} \begin{bmatrix} \dfrac{\partial f_2}{\partial y_r} & \dfrac{\partial f_2}{\partial \nu} \\ \dfrac{\partial f_4}{\partial y_r} & \dfrac{\partial f_4}{\partial \nu} \end{bmatrix} \begin{bmatrix} \mathrm{d}y_r \\ \mathrm{d}\nu \end{bmatrix} = \begin{bmatrix} 0 \\ 0 \end{bmatrix}. \tag{44}$$

For this equation to be zero, it suffices for the determinant of the 2×2 Jacobian matrix in the equation to be zero; that is,

$$f_7 = \begin{vmatrix} \dfrac{\partial f_2}{\partial y_r} & \dfrac{\partial f_2}{\partial \nu} \\ \dfrac{\partial f_4}{\partial y_r} & \dfrac{\partial f_4}{\partial \nu} \end{vmatrix} = 0. \tag{45}$$

Expanding and rearranging this determinant gives the following equation:

$$f_7 = 30x_r^{37} - 297x_r^{39} + 123x_r^{41} + 528x_5^{35}y_r^2 + \ll 59582\ \text{terms} \gg + 192y_r^{10}\zeta_1^3\mu^2\nu^{24} = 0. \tag{46}$$

Equations (42) and (46) constitute three simultaneous algebraic equations including the three unknowns x_r, y_r, and ν. These expressions can be solved by the Newton–Raphson method to obtain numerical solutions for x_r, y_r, and ν. By substituting these numerical solutions in Eqs. (41), (40), (39), and (38) in order, the optimal values of all parameters are obtained.

8.2. Optimal solution of dynamic vibration absorber by stability criterion

Figure 16 shows the stability-optimal design parameters for the DVA obtained by numerical analysis. In comparison with the optimal solutions for the parallel-type DVA based on the H_∞ and H_2 criteria discussed above, the stability criterion has the following two features.

(1) The optimal mass ratio $\mu_{B\mathrm{opt}}$ of the two DVAs is quite small, and it approaches zero as μ increases.

(2) The optimal damping ratios $\zeta_{2\mathrm{opt}}$ and $\zeta_{3\mathrm{opt}}$ are large.

8.3. Maximized stability

Figure 17(b) shows the maximized stability $\Lambda_{\max}$ for the primary system to which the parallel-type double-mass DVA optimized by the stability criterion is attached. For comparison, Fig. 17(a) shows the maximized stability for the series-type double-mass DVA. A comparison of these figures reveals that the optimized stability of the parallel-type DVA is much smaller than that of the series-type DVA and the increase in the stability with increasing primary system damping is also relatively small for the parallel type DVA. In particular, for large ζ_1, the reversal phenomenon occurs, which causes the stability to reduce as the mass ratio μ increases. In these plots, the results for $\mu = 0$ shown in gray indicate the stability of the primary system when no DVA is attached.

[DOI: 10.1299/mej.19-00051]

8.4. Frequency response of a system optimized by the stability criterion

Figures 18 and 19 show the compliance transfer functions of primary systems to which the series- and parallel-type DVAs are attached, respectively. When designing a DVA using the stability criterion, there is only one resonance point in the frequency response. The stability of the system with the parallel-type DVA is considerably lower than that of the system with the series-type DVA, and there are clear differences in the frequency responses of the system in the two cases.

9. Concluding remarks

The inclusion of damping in the primary system makes optimization of a DVA difficult, and even for a single-mass DVA, an exact optimal solution based on the H_∞ criterion has not been obtained. In a previous report (Asami, 2019), an exact algebraic solution for a series-type double-mass DVA has been reported for three optimization criteria (H_∞ optimization, H_2 optimization, and stability maximization). However, the present assessment indicates that there are 22 different solutions for the optimization of a double-mass DVA. In the present report, among the three transfer functions, the compliance transfer function was considered, and optimization of the series- and parallel-type double-mass DVAs was carried out based on the above three design criteria. Of the 10 different optimal solutions reported herein, almost all were obtained numerically by solving the exact simultaneous equations, except for two cases that had been reported previously.

In contrast to the optimization problems in which algebraic solutions were obtained, in the DVA optimization problems for which the simultaneous equations cannot be solved algebraically, changes in the optimal solution with respect to the primary system damping are drastic and complex. In other words, the optimal parameter values change quasi-linearly and gradually with respect to the primary system damping in the optimization problems for which algebraic solutions can be obtained, whereas the numerical solutions obtained in this report do not show similar trends.

The optimal design conditions for the parallel-type double-mass DVA attached to a damped primary system were first derived alongside those for the series-type DVA. The performance of the parallel-type DVA was found to be inferior to the series-type DVA under all optimization criteria. Although this performance comparison has already been reported for an undamped primary system (Asami et al., 2018), it was confirmed that the same can be said when there is damping in the primary system.

References

Asami, T., Nishihara, O., and Baz, A. M., Analytical Solutions to H_∞ and H_2 Optimization of Dynamic Vibration Absorbers Attached to Damped Linear Systems, ASME Journal of Vibration and Acoustics, Vol.124, No.2 (2002), pp.284-295.

Asami, T., and Nishihara, O., Closed-Form Solution to H_∞ Optimization of Dynamic Vibration Absorbers (Application to Different Transfer Functions and Damping Systems), ASME Journal of Vibration and Acoustics, Vol.125, No.3 (2003), pp.398-405.

Asami, T., Optimal Design of Double-Mass Dynamic Vibration Absorbers Arranged in Series or in Parallel, ASME Journal of Vibration and Acoustics, Vol.139, No.1 (2017), p.011015.

Asami, T., Erratum of "Optimal Design of Double-Mass Dynamic Vibration Absorbers Arranged in Series or in Parallel," ASME Journal of Vibration and Acoustics, Vol.140, No.2 (2018), p.027001.

Asami, T., Mizukawa, Y., and Ise, T., Optimal Design of Double-Mass Dynamic Vibration Absorbers Minimizing the Mobility Transfer Function, ASME Journal of Vibration and Acoustics, Vol.140, No.6 (2018), p.061012.

Asami, T., Exact Algebraic Solution of an Optimal Double-Mass Dynamic Vibration Absorber Attached to a Damped Primary System, ASME Journal of Vibration and Acoustics, Vol.141, No.5 (2019), p.051013.

Brock, J. E., A Note on the Damped Vibration Absorber, ASME Journal of Applied Mechanics, Vol.13, No.4 (1946), p. A-284.

Frahm, H., Device for Damping Vibrations of Bodies, U.S. Patent No. 989, 958 (1911), pp.3576-3580.

Hahnkamm, E., Die Dämpfung von Fundamentschwingungen bei veränderlicher Erregergrequenz, Ingenieur Archival, Vol.4 (1932), pp.192-201.

Ikeda, K., and Ioi, T., On the Dynamic Vibration Damped Absorber of the Vibration System, Bulletin of the JSME, Vol.21, No.151 (1978), pp.64-71.

Iwanami, K., and Seto, K., An Optimum Design Method for the Dual Dynamic Damper and Its Effectiveness, Bulletin of JSME, Vol.27, No.231 (1984), pp.1965-1973.

[DOI: 10.1299/mej.19-00051]

Kreyszig, E., Advanced Engineering Mathematics, 8th ed., (1999), p.784, John Wiley & Sons, Inc., New York.

Nishihara, O., and Matsuhisa, H., Design of a Dynamic Vibration Absorber for Minimization of Maximum Amplitude Magnification Factor (Derivation of Algebraic Exact Solution), Transactions of the JSME, Ser. C, Vol.63, No.614 (1997), pp.3438-3445, (in Japanese).

Nishihara, O., and Asami, T., Closed-Form Solutions to the Exact Optimizations of Vibration Absorbers (Minimizations of the Maximum Amplitude Magnification Factors), ASME Journal of Vibration and Acoustics, Vol.124, No.4 (2002), pp.576-582.

Nishihara, O., Minimization of Maximum Amplitude Magnification Factor in Designing Double-Mass Dynamic Vibration Absorbers (Application of Optimality Criteria Method to Parallel and Series Types), Transactions of the JSME, Vol.83, No.849 (2017), p.16-00549, (in Japanese).

Ormondroyd, J., and Den Hartog, J. P., The Theory of the Dynamic Vibration Absorber, ASME Journal of Applied Mechanics, Vol.50, No.7 (1928), pp.9-22.

Pan, G., and Yasuda, M., Robust Design Method of Multi Dynamic Vibration Absorber, Transactions of the JSME, Ser. C, Vol.71, No.712 (2005), pp.3430-3436, (in Japanese).

Randall, S. E., Halsted, D. M., and Taylor, D. L., Optimum Vibration Absorbers for Linear Damped System, ASME Journal of Mechanical Design, Vol.103, No.4 (1981), pp.908-913.

Sekiguchi, H., and Asami, T., Theory of Vibration Isolation of a System with Two Degrees of Freedom, Bulletin of the JSME, Vol.27, No.234 (1984), pp.2839-2846.

Soom, A., and Lee, M., Optimal Design of Linear and Nonlinear Vibration Absorbers for Damped System," ASME Journal of Vibration and Acoustics, Vol.105, No.1 (1983), pp.112-119.

Thompson, A. G., Optimum Tuning and Damping of a Dynamic Vibration Absorber Applied to a Force Excited and Damped Primary System, Journal of Sound and Vibration, Vol.77, No.3 (1981), pp.403-415.

Yasuda, M., and Pan, G., Optimization of Two-Series-Mass Dynamic Vibration Absorber and Its Vibration Control Performance, Transactions of the JSME, Ser. C, Vol.69, No.688 (2003), pp.3175-3182, (in Japanese).

Zuo, L., Effective and Robust Vibration Control Using Series Multiple Tuned-Mass Dampers, ASME Journal of Vibration and Acoustics, Vol.131, No.3 (2009), p.031003.

[DOI: 10.1299/mej.19-00051]